Investigation of petrophysical and rock physical aspects of CO_2 storage in sandstone reservoirs

An experimental study

Javad Naseryan Moghadam

Dissertation for the degree of Philosophiae Doctor (Ph.D.)

Faculty of Mathematics and Natural Sciences

Department of Geosciences

University of Oslo

Norway

September 2016

Series of dissertations submitted to the
Faculty of Mathematics and Natural Sciences, University of Oslo
No. 1795

ISSN 1501-7710

Cover: Hanne Baadsgaard Utigard.
Print production: Reprosentralen, University of Oslo.

Preface

This thesis is entitled 'Investigation of petrophysical and rock physical aspects of CO_2 storage in Sandstone reservoirs'. The thesis has been submitted to the Department of Geosciences at the University of Oslo in accordance with the requirements for the degree of Philosophiae Doctor (Ph.D) in Petroleum Geosciences. The study was performed as a part of the FME SUCCESS (Subsurface CO_2 storage – Critical Elements and Superior Strategy) project. It is a center for environment-friendly Energy Research (FME) that established cooperation between industry and academics in order to enhance the competence and fill knowledge gaps in the geological CO_2 storage. This work is funded by the University of Oslo and SUCCESS under grant 193825/S60 from the Research Council of Norway and hosted by Christian Michelsen Research (CMR). The main supervisor is Senior Researcher, Dr. Helge Hellevang and the co-supervisors are Assoc. Prof. Nazmul Haque Mondol and Prof. Emeritus Per Aagaard.

In the introduction part of the thesis, background information about CO_2 storage and its mechanisms are presented. In the second chapter, properties influencing CO_2 fluid flow, such as absolute permeability and its effective stress coefficient (α_k), wettability, capillary pressure and relative permeability, are discussed. The rock physical aspects of CO_2 storage and possibility for seismic monitoring of CO_2 plume movement inside the storage formation are also described. The published papers are summarized in the third chapter.

The main objective of this study was to investigate the rock physical and petrophysical aspects of CO_2 storage in sandstone reservoirs. The tested core plugs for this study were provided by the Longyearbyen CO_2 Lab, Svalbard, Norway (Knorringfjellet sandstone), Norwegian Geotechnical Institute (NGI) (Red Wildmoor sandstone) and Cleveland Quarries, Ohio, USA (Berea sandstone). The first part of the research, CO_2 rock physics, has been performed at the University of Oslo (UiO) and the Norwegian Geotechnical Institute (NGI), and the last two parts, CO_2 petrophysics-fluid flow, have been performed solely at the Department of Geosciences at University of Oslo. The work has resulted in three journal papers (two published and one under review), and three conference extended abstracts. In the first paper we reported the acoustic velocity behavior of CO_2 saturated sandstone under varying temperatures and pressures representing different CO_2 phases. In the second paper, the effective stress coefficient for the permeability (α_k) of sandstones is measured and modelled by presenting a *Modified Clay Shell Model* by applying spherical geometry instead of cylindrical geometry and utilizing both water and CO_2 as test fluids. In the third paper, the

relative permeability of CO_2-water systems in sandstones has been measured and modelled, and the associated impacts of rock heterogeneity, residual trapping and wettability and their implications on CO_2 storage are discussed. The three conference extended abstracts are presented in the appendix section that were provided based on the initial outcomes of this research.

To my beloved wife

&

The Love of my Life

Farxaneh

Most sincere gratitude and heartfelt thanks for your unconditional

Love

And support throughout the entire journey

Acknowledgements

First and foremost I would like to thank my supervisors Dr. Helge Hellevang, Associate Professor MD. Namul Haque Mondol and Professor Emeritus Per Aagaard for their guidance, understanding and patience and giving me the opportunity to start on this exciting study. Special thanks to Helge for his excellent advices, encouragement, supervision and contributions to the work. I am deeply grateful for our scientific discussions that helped me a lot during my research. Thanks to you Nazmul for always pushing me in the right direction, continuous support and having faith in me through these years. Per has been always an inspiration for me and many others by his kindness, support and guidance.

I would like to express my gratitude to the Department of Geosciences at University of Oslo (UiO), the Norwegian Research Council and the SUCCESS research center for funding this Ph.D. fellowship. Many thanks go to the members of the SUCCESS project specially Professor Alvar Braathen as the leader of the CO2LYB pilot project that helped me a lot by providing the required core samples from Svalbard area. I would also like to thank Norwegian Geotechnical Institute (NGI) for providing laboratory facilities and cooperating under the SUCCESS project. In addition, I would like to express my gratitude to CoreLab Company, specially, the senior CoreLab technician Ben Anderson for providing technical support for the AFS-200 flooding system at UiO.

I would also like to specially thank Beyene Girma Haile as a good friend and colleague that provided valuable guidance through these years. Thanks to you Gudmund for facilitating everything and your help. My thanks also go to my former and current office mates Binyam, Daniel and Lina. I would also like to thank Mohammad, Honore, Mohsen, Salah, Noora, Hossein, Irfan, Oluwakemi, Sirikaran and Amir as my good friends for their help and support. Furthermore I would like to thank Touraj Fathollahpour and his family that helped a lot by their kindness and support. Special thanks go to Geir Olav Aas and Katrin Kruse for their nice mood and kindness. I would also like to thank everyone who helped me and contributed through the entire journey.

I would like to thank my parents and my wife's parents. I express my sincere gratitude to Mahbobe, Reza, Kian and Amir Mohammad for unconditional support and love through these years. Last and not least I would like to express my deepest gratitude and sincere thanks to my beloved wife Farzaneh since if I wasn't supported by her unconditional love, help and encouragement, I would have never been able to accomplish the PhD journey. Special thanks to you my angel because of always believing me through the entire journey.

List of peer-reviewed journal papers

Paper I: **Naseryan Moghadam, J.**, Mondol, N.H., Aagaard, P. and Hellevang, H. 2016, Experimental investigation of seismic velocity behavior of CO_2 saturated sandstones under varying temperature and pressure conditions, Journal of Greenhouse Gases: Science and Technology, DOI: 10.1002/ghg.1603.

Paper II: **Naseryan Moghadam, J.**, Mondol, N.H., Aagaard, P. and Hellevang, H. 2016, Effective stress law for the permeability of clay bearing sandstones by the Modified Clay Shell Model, Journal of Greenhouse Gases: Science and Technology, DOI: 10.1002/ghg.1612.

Paper III: **Naseryan Moghadam, J.**, Mondol, N.H., Hellevang, H. and Aagaard, P. 2016, Determination of CO_2-brine relative permeability curves for the tight Knorringfjellet (Svalbard, Norway) and permeable Berea sandstones, submitted to International Journal of Greenhouse Gas Control, September 2016.

List of extended abstracts

Extended Abstract I: **Naseryan Moghadam, J.**, Mondol, N.H. and Aagaard, P. 2012, Evaluation of mechanical strength of a Barents Sea Shale by applying the most common failure criteria, Third EAGE Shale Workshop on Shale Physics and Shale Chemistry: New Plays, New Science, New Possibilities, 23-25 January 2012, Barcelona, Spain, DOI: 10.3997/2214-4609.20143917.

Extended Abstract II: **Naseryan Moghadam, J.**, Mondol, N.H., Hellevang, H., Johnsen, Ø. and Aagaard, P. 2014, Seismic response of CO_2 saturated Red Wildmoor Sandstone under varying temperatures and pressures, 76th EAGE Conference & Exhibition 2014, 16-19 June 2014, Amsterdam, Netherlands, DOI: 10.3997/2214-4609.20140849.

Extended Abstract III: **Naseryan Moghadam, J.**, Mondol, N.H., Hellevang, H. and Aagaard, P. 2014, Determination of the effective stress coefficient for the permeability of two low permeable sandstones in the Svalbard area, 4th Low Permeability Workshop, 29-30 September 2014, Ecole Centrale de Lille, France.

Table of Contents

1. Introduction

Utilization of fossil fuel for energy production results in large emissions of greenhouse gases including CO_2 that is believed to cause global warming and climate change. Capture and geological sequestration of the anthropogenic CO_2 emissions (CCS) is understood to be a reliable solution for overcoming the ascending trend of atmospheric CO_2 (Bachu, 2000; Benson et al., 2005; IEA, 2015; Skov et al., 2002). Among the proposed CO_2 sequestration sites, saline aquifers are considered as one of the most viable options due to their large storage capacities and availability when needed (Bennion and Bachu, 2005).

Several studies have been performed to understand the fate of subsurface CO_2 storage. One of the most important issues is the proper trapping of the injected CO_2 inside the target formation for an extended time to prevent it from reaching the atmosphere and polluting the surrounding formations. The considered CO_2 trapping mechanisms inside the target formation are structural and stratigraphical trapping, solubility trapping, residual trapping and mineral trapping (Firoozabadi and Cheng, 2010; Zhang and Song, 2014). Residual trapping during the imbibition cycle is the main focus of this study in which the in-situ fluid replaces the injected CO_2 and immobilizes a large portion of it (Juanes et al., 2006; Pentland et al., 2011).

Monitoring of the CO_2 plume inside the reservoir must be duly considered in order to avoid undesirable phenomena such as fracturing the sealing cap rock formations, reopening the existing fractures, reactivation of the faults and consequent CO_2 leakage due to high CO_2 injection pressures. Indirect monitoring techniques like seismic monitoring are preferred over direct monitoring techniques like drilling observation wells due to the cost and geomechanical integrity issues. Time-lapse seismic monitoring technique has been successfully applied for monitoring several enhanced oil recovery (EOR) operations for example McElroy field (West Texas, USA) and Weyburn-Midale field (Southeastern Saskatchewan, Canada) (Wang et al., 1998; Wang and Nur, 1989; White, 2009). It also has been utilized as the most important technique for monitoring CO_2 plume movement inside the reservoir for some CO_2 storage projects such as Sleipner (North Sea, offshore Norway) and In Salah CCS project (Central Algeria) (Arts et al., 2004; Ringrose et al., 2013). The seismic signature of the rock is a function of both rock and pore fluid bulk moduli and this can be utilized for monitoring CO_2 plume migration over time inside the target formation (Arts et al., 2004; Avseth et al., 2010; Mavko et al., 2009).

Although in reservoir the CO_2 coexists with in-situ pore fluid, detailed study of the end member of fully CO_2 saturated (100%) sandstone can provide better understanding of time-lapse seismic monitoring data.

Mechanical integrity of the target reservoir and the overlaying cap rock depends on the fluid pressure and the extent of CO_2 movement inside the reservoir. The fluid flow is strongly a function of porosity, absolute permeability, CO_2-brine relative permeability and wettability. Absolute permeability is an intrinsic property of the rock that might be greatly affected by pore pressure increase and consequently effective stress reduction during CO_2 injection (Streit and Hillis, 2004). Understanding relative permeability hysteresis due to multiple interstitial fluid distributions for each level of saturation is a key in determining the extent of the observed CO_2 residual trapping (Juanes et al., 2006). As a larger portion of the injected CO_2 is trapped residually, the risk of formation of CO_2 gas caps beneath the seal decreases and consequently the geomechanical integrity of the cap rock persists.

Studying the impact of petrophysical properties on CO_2-induced deformations should be properly considered for better understanding the risk of leakage through the seal. Experimental analysis of the rock physical aspects of CO_2 storage beside the petrophysical properties of the CO_2-water systems in laboratory conditions provide important insight for better understanding the fate of CO_2 at reservoir conditions.

1.1. Objectives and scope of the study

The present study was carried out to investigate the petrophysical and rock physical aspects associated with CO_2 storage in saline aquifers. The target reservoir is the Knorringfjellet formation that is recently considered as a potential for a pilot CO_2 sequestration project (CO2LYB) in Svalbard area in Norway. The purpose of running the CO2LYB pilot project was to evaluate the local geological conditions for subsurface sequestration of CO_2. The Longyearbyen area (Svalbard) is planned to be a CO_2 free society while the produced CO_2 by the coal burning power plant is planned to be sequestrated into the subsurface formations (Braathen et al., 2012). The Knorringfjellet sandstone is classified as rather tight and cemented rock with relatively low porosity and permeability (Farokhpoor et al., 2010; Mørk, 2013; Naseryan Moghadam et al., 2016a; Naseryan Moghadam et al., 2016b). It was aimed to provide rock physical-petrophysical data for CO_2-water saturated sandstone systems as very few studies were performed on this formation (Farokhpoor et al., 2012; Mørk, 2013). Tight rocks occur worldwide and the results from this study may be relevant for providing a better

insight for sandstone reservoirs with similar characteristics (highly cemented and tight formations) like equivalent formations in Barents Sea.

This study is divided into three sub tasks. The primary aim of the study under the first task was to analyze the effect of CO_2 phase transitions on seismic velocities (both V_p and V_s) of CO_2 saturated sandstones. Studying seismic signature of fully CO_2 saturated sandstone under reservoir condition was planned for providing a valuable assist in better interpretation of time-lapse seismic monitoring data. In addition, we aimed at analyzing the porosity impact on velocity linked to CO_2 phase transitions. This task was fulfilled by performing special tests and acquiring acoustic velocity data (both V_p and V_s) at NGI (Norwegian Geotechnical Institute) rock physics laboratory under varying CO_2 temperature and pressure conditions representing different thermo-physical CO_2 states. The utilized materials in this task were the Knorringfjellet and Red Wildmoor sandstone core plugs.

In the second task, it was attempted to address the relative impact of parameters like confining stress and pore pressure on absolute permeability of sandstone formations in the form of an *effective stress law*. This part of the study integrated the pore pressure increase with the reduction of effective stress during CO_2 injection and its implication on the storage integrity. It was also aimed to present a modified model for better fitting the observed effective stress coefficients for the permeability (α_k) by considering spherical geometry instead of commonly applied cylindrical geometry. These aims were pursued by performing absolute permeability measurements on sandstone samples (Knorringfjellet and Berea) under varying confining stress (σ_c) and pore pressure (P_p) conditions and utilizing water and CO_2 as test fluids.

In the third task, the relative permeability (K_r) of CO_2-water systems in tight sandstones and the impact of the associated parameters like heterogeneity and wettability on K_r has been investigated. Furthermore, the role of the observed relative permeability hysteresis on residual CO_2 trapping mechanism has been discussed. Analyzing the K_r behavior of gaseous CO_2-water system instead of supercritical CO_2 and implication of the relative permeability hysteresis and consequent CO_2 trapping on geomechanical integrity of the sealing cap rock was another matter of interest. The above-mentioned goals were achieved by performing *unsteady state* drainage and imbibition relative permeability experiments on two (Knorringfjellet and Berea) sandstone samples.

In order to accomplish the targeted research goals in the task 1, two extended abstracts were provided. In the first extended abstract, the application of the most common mechanical failure criteria for prediction of the maximum effective principal stress (σ_1) of Barents Sea shale samples from Hekkingen formation is investigated. Shales and mudrocks are the most

common seals that prevent migration of the in-situ hydrocarbon and injected CO_2. Reliable prediction of the maximum sustainable stress is quite essential in order to avoid risking geomechanical integrity of the overlaying cap rock due to injection of large magnitudes of high-pressure CO_2. In the second extended abstract, the initial obtained results from the performed rock physical experiments on Red Wildmoor sandstone saturated with CO_2 at different thermodynamic states are presented. The possibility of monitoring CO_2 phase transition in reservoir condition was also discussed. The second task was followed by presenting the third extended abstract in which the relative impact of confining stress and pore pressure on the observed permeability values and their associated effective stress coefficients for the permeability were studied. The utilized core plugs were selected from Knorringfjellet and DeGeerdalen sandstone formations in Svalbard area in order to investigate effective stress change due to the CO_2-induced pore pressure increase.

2. Scientific background

2.1. Geological CO_2 sequestration

Increasing world's population and rapid economic growth especially in developing countries have resulted in increasing energy consumption and emissions of greenhouse gases like CO_2 into the surrounding environment. It is of major concern that this may cause global warming and climate changes (Benson et al., 2005; IEA, 2015). Capturing large amounts of CO_2 and its storage (CCS) into the underground geological formations is proposed for mitigating increasing atmospheric CO_2. The common storage sites considered for CO_2 sequestration are deep saline aquifers, depleted oil and gas reservoirs, unminable coal seams, basalts and oil shales (Bachu et al., 2007; Benson et al., 2005; Cook, 1999) (Figure 1).

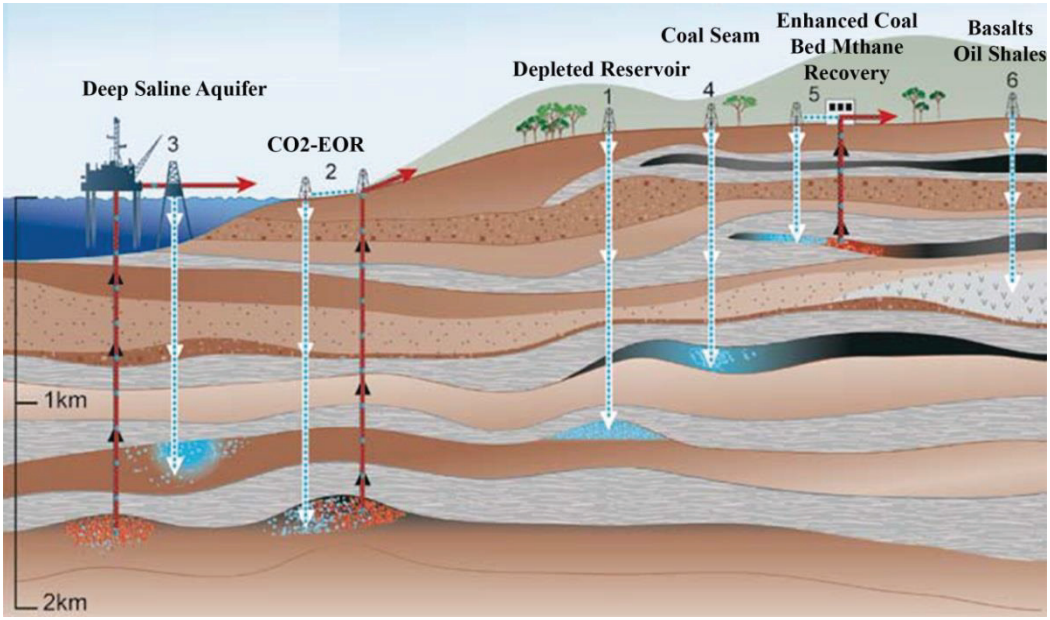

Figure 1: CO_2 EOR and storage scenarios, modified after (Cook, 1999)

Deep saline aquifers are considered to be one of the best CO_2 storage options due to their large storage capacity, worldwide distribution, availability upon the time of injection and not being exposed for surface usage (Bennion and Bachu, 2005). Although the process of capturing CO_2 from large stationary sources like power plants and oil refineries and underground storage is costly, considering tax credits and regulations regarding environmental fines or considering CO_2 for EOR purposes may make the investment on CCS justifiable (Hellevang, 2015).

The main CO_2 storage mechanisms are structural-stratigraphical (hydrodynamic), residual, solubility and mineral trapping (Zhang and Song, 2014) (Figure 2). The injected supercritical CO_2 is more buoyant than the in-situ pore fluid and therefore percolates up through the pore space. Hydrodynamic trapping is the most dominant trapping mechanism in which the CO_2 is trapped after it reaches the impermeable overlaying caprock. The buoyancy contrast between CO_2 and the in-situ pore fluid, and consequent upward migration of the injected CO_2, results in formation of a CO_2 plume beneath the overlaying cap rock.

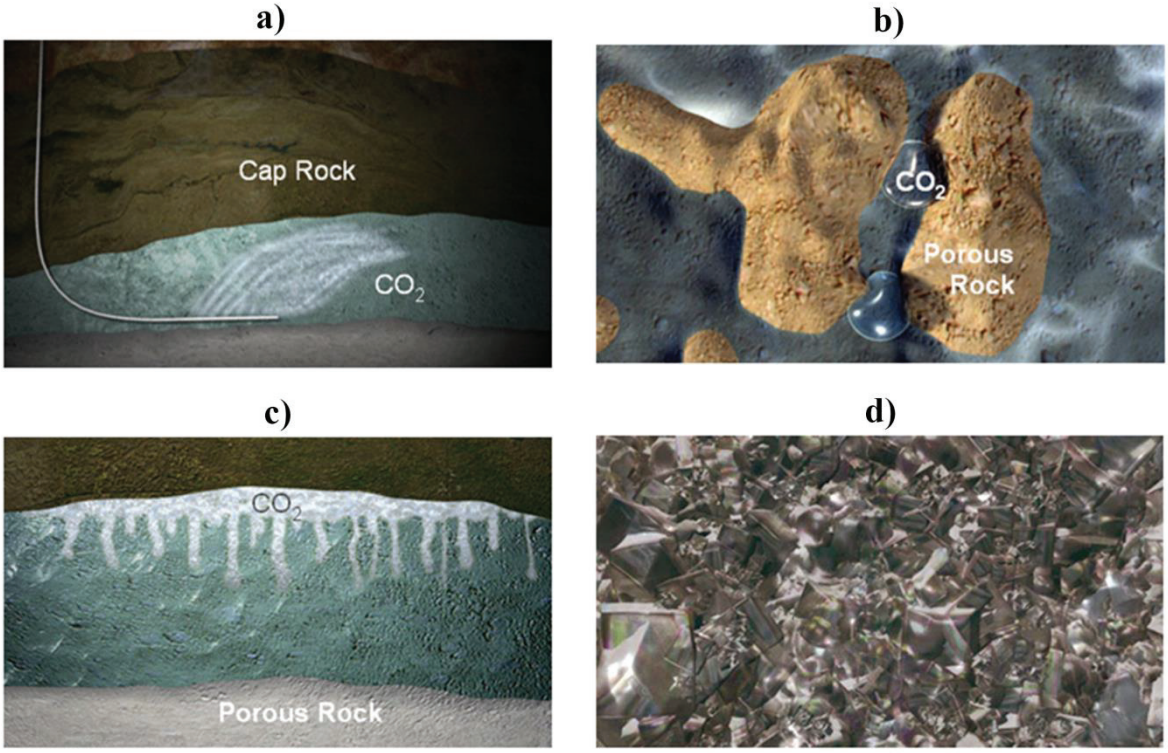

Figure 2: CO_2 storage mechanisms a) Structural-stratigraphical, b) Residual, c) Solubility and d) Mineral trapping (modified after (CO2-Capture-Project, 2015))

A portion of the injected CO_2 can be permanently stored by dissolution in the in-situ brine in both gaseous and supercritical states. Temperature, pressure and salinity are the factors that determine the extent of CO_2 dissolution (0.9-3.6 *mol*%) into the formation brine (Kiepe et al., 2002). CO_2 dissolution into the formation brine during imbibition is faster compared to the initial drainage as the contact area per volume of the individual trapped CO_2 bubbles is considerably larger. The CO_2 saturated brine is heavier than the in-situ brine and may therefore induce gravitational flow instabilities in the reservoir. The CO_2 saturated brine may then sink to the bottom of the reservoir over hundreds to thousands of years and the density-

driven convection may leads to formation of thick and thin fingers. This will further accelerate the CO_2 entrapment. However the advancement of the mentioned fingers due to convective mixing inside the reservoir may be limited due to existence of heterogeneity as heterogeneity reduces the instability of the system (Bjørlykke et al., 1988; Chen et al., 2013; Iglauer, 2011; Riaz et al., 2006).

The injected CO_2 and formation brine react and form carbonic acid that lowers the *pH* of the brine. The increased acidity destabilizes formation minerals and leads to dissolution. The released cations may further react with dissolved CO_2 over a period of time and form carbonate minerals that precipitate. The rate of the mentioned reaction is strongly depending on the chemistry of the in-situ water and the mineralogy of the storage formation (Hellevang et al., 2013).

The mentioned chemical reactions between the formed carbonic acid and the in-situ minerals in the surrounding environment especially in carbonate reservoirs may result in formation of high permeability channels. The flow channels are preferred by the injected CO_2 as the flow pathway. This phenomenon reduces capillary trapping of CO_2 as achieving lower initial CO_2 saturation during drainage cycle results in lower trapped CO_2 saturation. Further dissolution of host rock may put the mechanical stability of the rock at risk. Precipitation of the formed carbonate minerals may introduce injection complexity due to blockage of small pore throats and consequent permeability reduction (Iglauer, 2011; Pentland et al., 2011).

The injected CO_2 will displace the in-situ brine during the drainage cycle and then will be replaced by the in-situ brine during the imbibition process. A portion of the CO_2 will be immobilized inside the pore space due to the existence of multiple interstitial fluid distributions for each level of saturation or permeability hysteresis (Honarpour and Mahmood, 1988; Oak et al., 1990). This phenomenon results in discontinuities in the CO_2 phase and formation of trapped CO_2 bubbles (Figure 3). The amount of trapped CO_2 inside the pore space is a function of reservoir rock-fluid properties, initial achieved CO_2 saturation during the drainage cycle, reservoir heterogeneity and wettability (Juanes et al., 2006; Pentland et al., 2011). Among all these trapping mechanisms, the residual trapping mechanism acts relatively faster compared to the others, within days to months, and is assumed to play an important role in trapping the sequestrated CO_2 within the first decades (Burnside and Naylor, 2014; Pentland et al., 2011; Sifuentes et al., 2009).

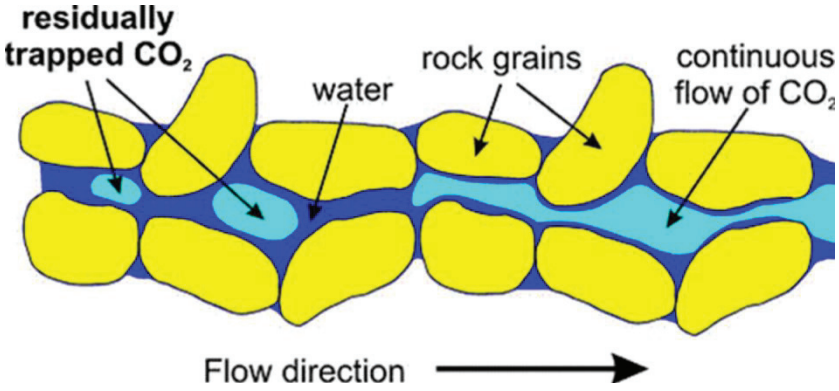

Figure 3: CO_2 residual trapping (Benson et al., 2005)

2.2. Monitoring

The CO_2 plume exerts vertical stress to the overlaying cap rock that is proportional to the height of the CO_2 plume. If the exerted vertical stress by the CO_2 plume exceeds the capillary forces in the overlaying caprock, mechanical failure and consequent CO_2 leakage through the induced pathway are expected (Busch and Amann-Hildenbrand, 2013; Rutqvist et al., 2007). The movement of the CO_2 plume must be monitored in order to evaluate the CO_2 trapping, locate the possible leakage pathways and determining the current thermo-physical state of the injected CO_2. Direct monitoring of the injected CO_2 by drilling observation wells is not recommended due to high costs, being time consuming and putting the geomechanical integrity of the sealing cap rock at risk. Indirect surveillance as seismic monitoring is an integral component of a controlling program that has been successfully utilized for monitoring the fluid movement in both CO_2 storage and enhanced oil recovery (EOR) (Lazaratos and Marion, 1997; Wang and Nur, 1989; White, 2009). Seismic behavior of a geological formation is controlled by both mineralogical composition-petrophysical properties of the formation and properties of the in-situ pore fluids (Batzle and Wang, 1992; Gassmann, 1951). The injected CO_2 significantly alters the seismic signature of the host formation due to considerable contrast between the physical-seismic properties of the in-situ pore brine and CO_2 that makes qualitative tracking and monitoring of the CO_2 plume migration possible (Gutierrez et al., 2012).

Time-lapse seismic monitoring is considered as a promising technique for monitoring the CO_2 plume migration inside the target reservoir (Arts et al., 2004; Chadwick et al., 2010; Ringrose et al., 2013). The time-lapse surface seismic monitoring at the Sleipner CO_2 storage operation over the last 20 years (from 1996) has provided an excellent example of application of this technique for monitoring CO_2 plume migration over time (Chadwick et al., 2010; Hellevang,

2015). Valuable objectives such as tracking the plume migration and understanding of fluid flow processes that control the CO_2 plume development within the target formation can be attained by performing time-lapse seismic monitoring (Chadwick et al., 2010).

2.3. Rock physical aspects of the CO_2 sequestration

Maximizing the CO_2 injectivity inside the target formation is highly desirable, but geomechanical limitation of reaching maximum sustainable formation pressure resulting in formation fracturing must also be considered. CO_2-water density contrasts results in upward migration of the injected CO_2 and formation of high pressure gas cap beneath the sealing cap rock. This exerts an upward pressure on the seal proportional to the height of the gas cap. The induced CO_2 over-pressurization may result in reopening of existing fractures, activation of faults and new fractures generation and consequent CO_2 leakage. This may put the geomechanical integrity of the sealing cap rock at risk (Arts and Winthaegen, 2005; Beaubien et al., 2005). Supercritical CO_2 is preferred for injection and sequestration due to its higher density and consequently for effective sweeping. The CO_2 can be present in gas, liquid and supercritical states and the required temperature and pressure conditions for its phase transition is reachable within the uppermost kilometer of the sedimentary basin (Lemmon et al., 2011; Yam and Schmitt, 2011) (Figure 4).

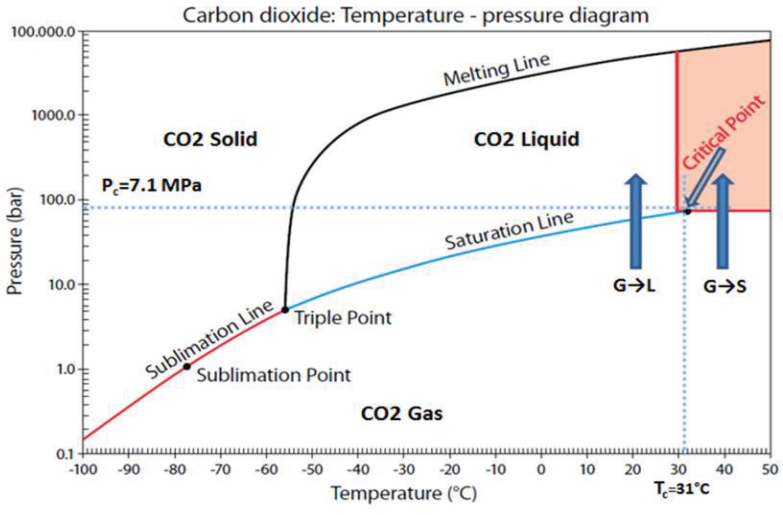

Figure 4: CO_2 phase diagram. The blue arrows illustrate gas (G) to liquid (L) and gas (G) to supercritical (S) state transitions for CO_2 (Modified after (Hunter, 2010; Leitner, 2000)). No phase boundary in case of G→S

The seismic response of a rock is not only a function of the mineralogical composition of the rock but is also affected by rock porosity, pressure and in-situ fluid properties (Mukerji and

Mavko, 1994; Wang and Nur, 1989). In order to determine the seismic velocities of a saturated rock the following relations are utilized (Mavko et al., 2009):

$$V_p = \sqrt{\frac{K_{sat}+4/3\mu}{\rho_{sat}}} \quad (1)$$

$$V_s = \sqrt{\frac{\mu}{\rho_{sat}}} \quad (2)$$

In which V_p and V_s are the compressional and shear wave velocities of the saturated rock respectively, K_{sat} is the bulk modulus of the saturated rock, ρ_{sat} is density of the saturated rock and μ is the shear modulus. Shear modulus of a saturated rock is the same as the dry rock as fluids cannot sustain shear forces:

$$\mu_{sat} = \mu_{dry} \quad (3)$$

Saturated density of the rock is defined as:

$$\rho_{sat} = (1-\varphi)\rho_s + \varphi\rho_f \quad (4)$$

In this relation, ρ_s and ρ_f are solid grain and pore fluid densities respectively. One of the most widely used fluid substitution equations in rock physics is the Gassmann equation (Gassmann, 1951). It relates the bulk modulus of a saturated rock (K_{sat}) to the bulk modulus of rock frame (K_{dry}), the mineral grain bulk modulus (K_s), the bulk modulus of the pore fluid (K_f) and the rock porosity (Mavko et al., 2009).

$$\frac{K_{sat}}{K_s-K_{sat}} = \frac{K_{dry}}{K_s-K_{dry}} + \frac{K_f}{\varphi(K_s-K_f)} \quad (5)$$

The K_{sat} of a rock that is saturated by fluid number 1 can be calculated when we know the K_{sat} of the same rock that is saturated with the fluid number 2:

$$\frac{K_{sat1}}{K_s-K_{sat1}} - \frac{K_{f1}}{\varphi(K_s-K_{f1})} = \frac{K_{sat2}}{K_s-K_{sat2}} - \frac{K_{f2}}{\varphi(K_s-K_{f2})} \quad (6)$$

Gassmann equation is only valid at low frequency and is based on several assumptions like isotropic behaviour of the porous material, well connectivity of the pore space, remaining in

closed system condition, constant porosity during fluid substitution and not being exposed to geochemical reactions and consequent phenomena like cementation and dissolution (Avseth et al., 2010; Mavko et al., 2009).

It is shown that the seismic response of the CO_2 saturated sandstone is affected by the CO_2/water ratio inside the pore space as it determines the saturated bulk modulus of the rock (Gutierrez et al., 2012; Shi et al., 2007; Wang and Nur, 1989). The increasing CO_2 saturation during injection period results in decreasing V_p while the V_s remains almost unchanged. This phenomenon is attributed to the reduction of the fluid bulk modulus and rock bulk density. Introducing CO_2 into a dry core is attributed to significant reduction of seismic velocities due to significant bulk modulus reduction around the critical pressure in which the CO_2 phase transition occurs (Chowdhury and Schmitt, 2013; Njiekak et al., 2013; Yam and Schmitt, 2011).

The observed velocity alteration is smoother at higher temperature in which the CO_2 gas to supercritical state transition takes place due to similarity between the physical properties of gaseous and supercritical states of CO_2 (No phase boundary is crossed). The observed velocity reduction is more abrupt at lower temperature due to significant contrast between the physical properties of gaseous and liquid CO_2 phases. The N_2 and H_2O saturated sandstone core plugs have not demonstrated any significant velocity alteration within the pressure interval in which CO_2 experiences phase transition (Njiekak et al., 2013). The obtained results also confirmed that Gassmann equation can be successfully utilized for modelling the seismic response of CO_2-brine and fully CO_2 saturated sandstones.

2.4. Impact of pore pressure and confining stress on absolute permeability

2.4.1. Absolute permeability

Reservoir rock properties are important parameters, which determine the success of in-situ hydrocarbon recovery and/or CO_2 sequestration accomplishment. Absolute permeability is one of the most important dynamic petrophysical properties of the reservoir rock and understanding the spatial variability of permeability plays a crucial role in reservoir simulation studies. Darcy (Darcy, 1856, 1857) reported that the observed water flux through the sand filters is directly proportional to the hydraulic pressure gradient resulting from water columns acting upon the sand column. For the laminar flow of the incompressible fluid through isotropic porous media the Darcy's concept can be written as (Ahmed, 2010b; Dake, 1983):

$$q = \frac{KA(P_{in}-P_{out})}{\mu L} \quad (7)$$

In which K is the absolute permeability (Darcy) (1 Darcy = $9.87.10^{-13}$ m^2), q is the flow rate (cm^3/sec), A is the cross section area of flow (cm^2), P_{in} and P_{out} are core inlet and outlet pressures respectively (atm), μ is the pore fluid viscosity (cp) and L is the length of the core (cm). In case of compressible fluid flow (gas), the equation is modified to account for compressibility:

$$q_m = \frac{KA}{\mu L} \cdot \frac{(P_{in}^2-P_{out}^2)}{2P_m} \quad (8)$$

Where the q_m is the measured flow rate at selected measurement pressure (P_m) (Ahmed, 2010a; Dake, 1983; Klinkenberg, 1941). The interaction between the gas molecules and capillarity is considered as the driving force for gas molecules in the direction of flow while mean free path of the gas (γ) is defined as the distance that gas molecules travel between successive molecular collisions. The higher gas permeability at lower pressures is attributed to higher mean free path of the gas (γ) that leads to gas slippage (Klinkenberg, 1941).

2.4.2. Effective stress coefficient for the permeability (α_k)

As a result of hydrocarbon recovery, the reservoir pore pressure (P_p) decreases and the effective stress ($\sigma_e = \sigma_c - P_p$) increases. This leads to decreasing reservoir permeability and hydrocarbon production rates (Zoback and Byerlee, 1975). The opposite is true during CO_2 storage where increasing in-situ pore pressures are accompanied by σ_e reduction and increase in permeability (Rutqvist et al., 2007). Decreasing permeabilities with increasing σ_c have been observed for different sandstones (Brace, 1978; Gray and Fatt, 1963; Thomas and Ward, 1972; Wyble, 1958). The mentioned phenomena make application of the effective stress law for describing permeability behavior of sandstones justifiable in which the permeability is considered as a function of both σ_c and P_p (Bernabe, 1986):

$$K = f(\sigma_e) = f\left(\sigma_c - \alpha_k P_p\right) \quad (9)$$

In which α_k is the effective stress coefficient for the permeability. Bernabe (Bernabe, 1987) defined α_k as the ratio between the permeability variation due to the change in applied P_p at constant σ_c and the permeability variation due to the change in applied σ_c at constant P_p:

$$\alpha_k = -\frac{\left(\frac{\partial k}{\partial P_p}\right)_{\sigma_c}}{\left(\frac{\partial k}{\partial \sigma_c}\right)_{P_p}} \tag{10}$$

α_k can be utilized for comparing the sensitivity of the rock permeability to the applied P_p and σ_c (Bernabe, 1986). Al-Wardy and Zimmerman (Al-Wardy and Zimmerman, 2004) suggested analyzing the pore radius (r) behavior in case of varying P_p and σ_c for calculating the α_k:

$$\alpha_k = -\frac{\left(\frac{\partial k}{\partial P_p}\right)_{\sigma_c}}{\left(\frac{\partial k}{\partial \sigma_c}\right)_{P_p}} = -\frac{\left(\frac{\partial k}{\partial r}\right)\left(\frac{\partial r}{\partial P_p}\right)_{\sigma_c}}{\left(\frac{\partial k}{\partial r}\right)\left(\frac{\partial r}{\partial \sigma_c}\right)_{P_p}} = -\frac{\left(\frac{\partial r}{\partial P_p}\right)_{\sigma_c}}{\left(\frac{\partial r}{\partial \sigma_c}\right)_{P_p}} \tag{11}$$

Utilizing α_k for expressing the permeability of rocks add simplicity to the permeability calculations by reducing the number of independent parameters to one (σ_e). α_k is normally calculated by utilizing Walsh cross-plot technique (Walsh, 1981) in which the permeability of the sample is measured at constant P_p and varying σ_c. Then the iso-perm lines are drawn and the correspondent σ_c and P_p are cross-plotted while α_k is the slope of the cross-plot (Figure 5).

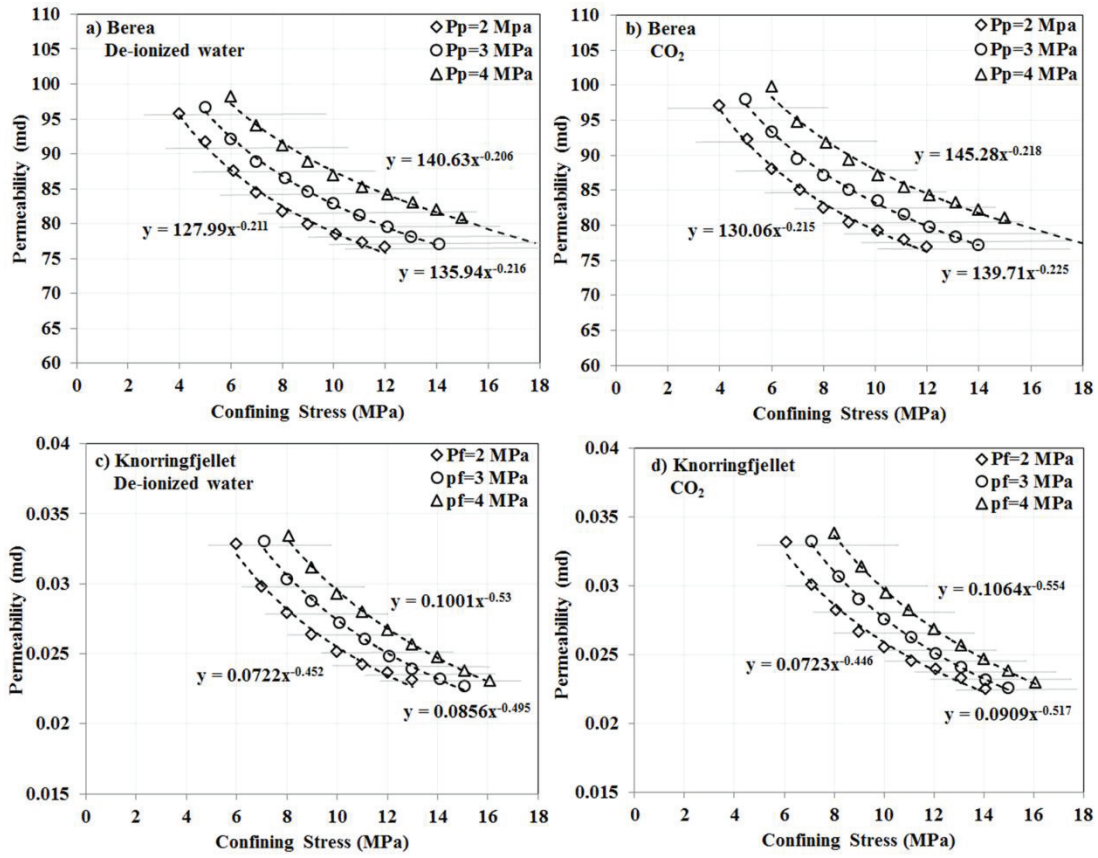

Figure 5: Observed permeability values at different σ_c and constant P_p for (a) Berea-water, (b) Berea-CO_2, (c) Knorringfjellet-water, and (d) Knorringfjellet-CO_2. The iso-perm lines are indicated on permeability-σ_c cross-plots as horizontal dashed lines (Naseryan Moghadam et al., 2016)

The α_k of mono-mineralogical rocks is calculated to be between rock porosity (φ) and 1.0 while the higher α_k values are attributed to the presence of rock heterogeneity due to clay

minerals inside the pore space (Berryman, 1992; Berryman, 1993). Depending on the percentage of clay content inside the sandstone (η), α_k values from 1 ($\eta \approx 0$) up to 7.1 ($\eta \approx 0.20$) have been reported (Walls and Nur, 1979; Zoback and Byerlee, 1975).

Large α_k values in case of clay bearing sandstone is described by Zoback and Byerlee (Zoback and Byerlee, 1975) by presenting the *Clay Shell Model*. They assumed that the granular framework of the pore space (quartz skeleton) is uniformly permeated by clay minerals in form of hollow cylinders (Figure 6). Significant contrast between the elastic moduli of quartz and clay minerals is reported (Mavko et al., 2009; Mondol et al., 2008; Woeber et al., 1963). Based on *Clay Shell Model*, the low compressible quartz grains are exposed to σ_c while the P_p is supported by the compressible clay. The mentioned phenomenon results in higher sensitivity of the clay to the applied P_p compared to σ_c and consequent $\alpha_k > 1$. In the *Clay Particle Model*, the higher sensitivity of the clay particles that are considered to be tangentially attached to pore walls to the applied P_p is assumed to be the reason behind large α_k values (Al-Wardy and Zimmerman, 2004) (Figure 6).

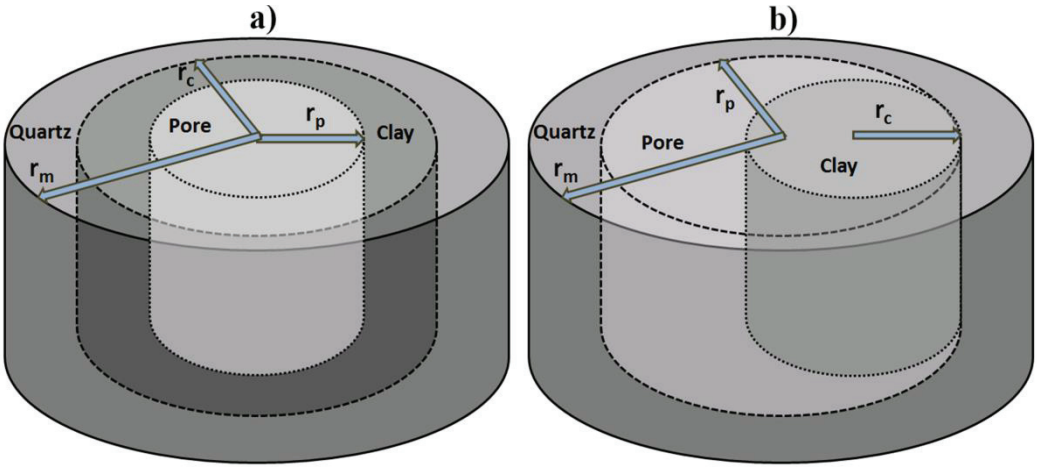

Figure 6: a) The presented *Clay Shell Model* by Zoback and Byerlee (1975) and b) *Clay Particle Model* by Al-Wardy and Zimmerman (2004). r_p, r_c and r_m are pore, clay and matrix radii respectively (Naseryan Moghadam et al., 2016).

2.5. Multi-phase flow and relative permeability of the CO_2-brine systems

Reservoir simulation software utilize the petrophysical data as input to predict the flow behavior and the provided data are regarded as a basis for reservoir management and well planning. The petrophysical properties are normally calculated in core laboratories by utilizing precise methodologies. Inaccurate estimation of these properties might lead to inaccurate prediction of original oil in place (OOIP) and hydrocarbon resources, maximum

CO_2 injectivity, water-cuts and selecting wrong production and EOR strategies. In order to study the multi-phase fluid flow through porous media in detail, the associated petrophysical properties of the rock such as capillary pressure (P_c), wettability, relative permeability (K_r) and residual trapping phenomenon must be understood. A brief description of the mentioned parameters is presented below:

2.5.1. Capillary pressure (P_c)

A discontinuity between the pressures of two immiscible fluids across the separating interface exists that is called capillary pressure. In case of CO_2-water system it's defined as (Ahmed, 2010b):

$$P_c = P_{CO2} - P_w \tag{12}$$

in which CO_2 is considered as the non-wetting phase. It can be calculated as:

$$P_c = \frac{2\sigma cos\theta}{r_p} \tag{13}$$

σ is the interfacial tension between fluids (dynes/cm), θ is the wettability angle, r_p is the effective pore radius (cm) and P_c (capillary pressure) is in dynes/cm^2. A typical P_c curve for the drainage (displacing wetting phase by non-wetting phase) and imbibition (displacing non-wetting phase by wetting phase) cycles is shown in figure 7. P_e or the threshold pressure is the minimum required pressure for the non-wetting phase to enter the porous medium. Capillary pressure data are utilized for evaluation of absolute and relative permeability, thickness of the transition zone and cap rock sealing capacity.

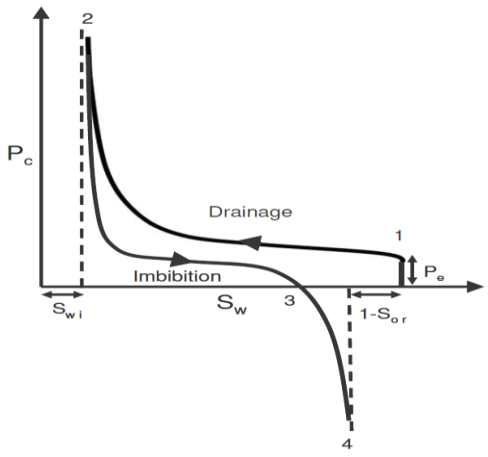

Figure 7: P_c curve for drainage and imbibition cycles (Amyx et al., 1960)

2.5.2. Rock wettability

Rock wettability is the measure of which phase preferentially adheres to the rock surface and is an important parameter in final recovery and EOR computations. When the wettability

angle for a fluid drop is less than 90°, the system is called wetting with respect to that fluid while a large wettability angle (≈180°) indicates that fluid isn't wetting (Figure 8).

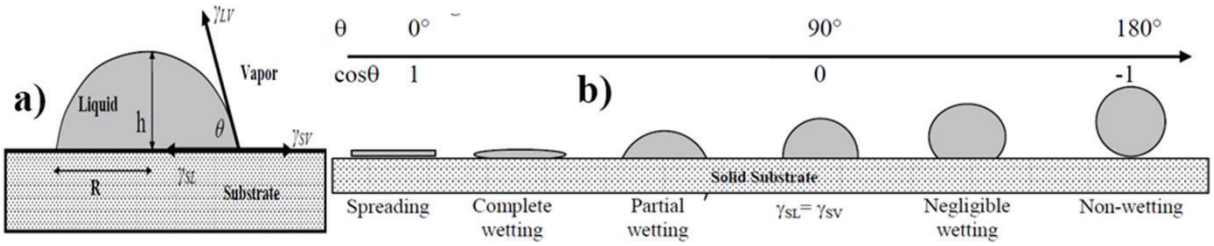

Figure 8: a) Contact angle definition, γ_{SL}, γ_{SV}, and γ_{LV} are solid-liquid, solid-vapor and liquid-vapor interfacial tensions b) Demonstrated different wettability conditions (Njobuenwu et al., 2007)

Most of the hydrocarbon reservoirs are water-wet prior to oil migration and the saturation profile is strongly a function of the initial and altered wettability (Abdallah et al., 1986). The water wettability of some sandstones like Berea in case of CO_2-water two phase flow is previously mentioned (Pentland et al., 2011).

2.5.3. Relative permeability

Normally more than one fluid is involved in case of fluid flow through porous media while the mobility of each fluid is affected by presence of other fluids. Fluid flow preference in case of simultaneous flow of multiple fluids is expressed by the relative permeability concept. The Darcy's law in case of simultaneous flow of water and CO_2 inside the pore space and considering the capillary pressure (P_c) is (modified after Amyx et al., 1960):

$$q_{CO_2} = -\frac{K_{CO_2}A}{\mu_{CO_2}}\left(\frac{\partial P_{CO_2}}{\partial x} + \Delta\rho g sin\theta\right) \quad (14)$$

$$q_w = -\frac{K_w A}{\mu_w}\left(\frac{\partial P_w}{\partial x} + \Delta\rho g sin\theta\right) \quad (15)$$

K_w and K_{CO2} represent effective water and CO_2 permeabilities respectively while θ is the angle between the core and the horizontal level. In case of horizontal flow through an isotropic medium, the relative permeability (K_r) is defined as the ratio of the effective permeability to the absolute permeability (K):

$$K_{rw} = \frac{q_w \mu_w L}{AK(P_{in} - P_{out})} \quad (16)$$

$$K_{rCO_2} = \frac{2q_{mCO_2}\mu_{CO_2}LP_m}{AK(P_{in}^2 - P_{out}^2)} \quad (17)$$

A typical drainage and imbibition K_r curve is illustrated in figure 9. As illustrated in this figure, the observed K_r curves for the drainage (displacement of the wetting phase by non-wetting phase) and imbibition (displacement of the non-wetting phase by wetting phase) cycles are not the same. During the imbibition cycle, a portion of the non-wetting phase will be immobilized inside the pore space due to existence of multiple interstitial fluid

distributions for each level of saturation that is called permeability hysteresis (Amyx et al., 1960; Honarpour and Mahmood, 1988; Oak et al., 1990).

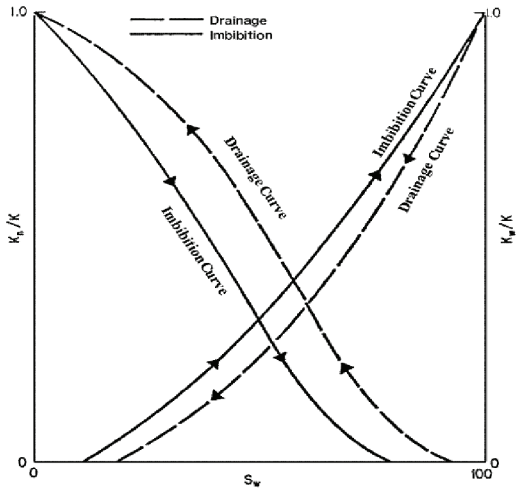

Figure 9: Typical relative permeability curve - hysteresis phenomenon (Amyx et al., 1960)

Relative permeability of a two phase flow system can be experimentally measured by *steady state* or *unsteady state* fluid displacement methods. In the *steady state* method, two phases are injected simultaneously at several fixed q_w/q_{nw} ratios until the steady state condition is achieved. Then, at each specific saturation, K_r of each phase based on its observed fractional flow is drawn (Abaci et al., 1992). In the *unsteady state* method the core is 100% saturated with one fluid and then the in-situ fluid is displaced with injecting another fluid. Injecting the displacing fluid is continued until no more production of the initial fluid is observed, indicating that the irreducible saturation of the initial fluid has been reached. Defining fractional flow of wetting and non-wetting phases as $f_w=q_w/q_t$ and $f_{nw}=q_{nw}/q_t$ respectively and neglecting the effect of capillary pressure results in the fractional flow equations:

$$f_w = \frac{1}{1+\frac{k_{rnw}\ \mu_w}{k_{rw}\ \mu_{nw}}} \tag{18}$$

$$f_{nw} = 1 - f_w \tag{19}$$

In case of CO_2-water systems, the fractional flow of water at the outlet in case of drainage can be estimated from the slope of the plot of gas saturation versus injected gas volume (Welge, 1952):

$$f_w = \frac{d\bar{S}_{CO2}}{d\bar{Q}_{CO2}} \tag{20}$$

While the average CO_2 saturation can be estimated by dividing cumulative produced volume of water (N_p) to the initial pore volume (V_p):

$$\bar{S}_{CO2} = \frac{N_p}{V_p} \tag{21}$$

The ratio K_{rCO2}/K_{rw} can be calculated by combining equations 18-21. Furthermore, by utilizing the calculated K_{rCO2} estimated from the injected volume of CO_2 during defined time intervals, the K_{rw} can be calculated. In comparison with the *steady state* method, the *unsteady state* method is less time consuming as it does not need flow rate-pressure drop stabilization and it is possible to estimate the irreducible water saturation (S_{wi}) (Abaci et al., 1992; Johnson et al., 1959). A typical CO_2-water relative permeability curve for sandstones is presented in figure 10. The water permeability at its 100% saturation is considered 1.0 whereas introducing a small amount of CO_2 into the core plug results in significant K_{rw} reduction.

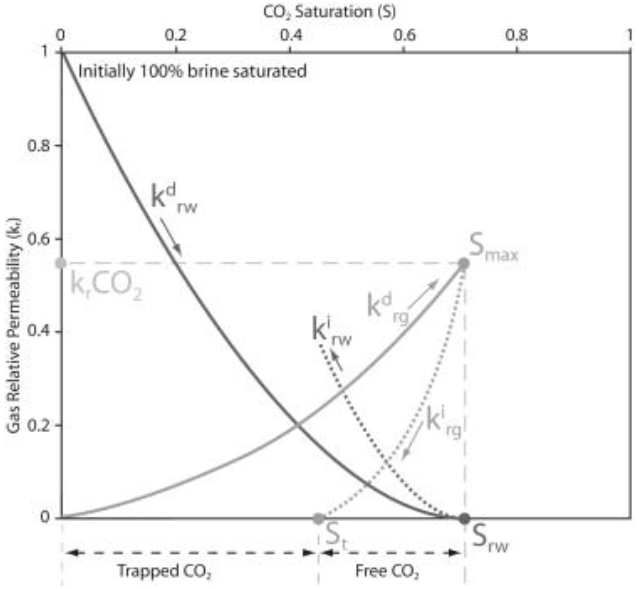

Figure 10: A general CO_2-water drainage and imbibition K_r curve (Burnside and Naylor, 2014)

The CO_2-brine relative permeability behavior is previously studied by performing displacement experiments on different sandstones (Bennion and Bachu, 2005; Burnside and Naylor, 2014; Krevor et al., 2012; Ruprecht et al., 2014). It is also observed that the fractional flow of CO_2 (f_{CO2}) at the core outlet during the drainage cycle is very high at relatively high water saturations. It means that by introducing a small amount of CO_2, while the major portion of the in-situ water is not displaced, the core outlet flow becomes just CO_2. The observed end-point CO_2 relative permeability at the end of the drainage stage has also been shown to be relatively low [$0.11<K_{rCO2}<0.54$] (Bennion and Bachu, 2005; Burnside and Naylor, 2014; Krevor et al., 2012; Ruprecht et al., 2014). This can be regarded as a clear indication of the water-wet nature of sandstones (Ahmed, 2010b). CO_2 (non-wetting fluid) occupies the larger pores and the water (wetting agent) fills the smaller pores that causes fluid flow to take place just in a small portion of the pore space. By further increasing the CO_2 saturation in drainage cycles, discontinuities in the wetting phase (water) take place leading to significant decrease in K_{rw}. The relatively low values of CO_2 end-point data (S_{CO2} and K_{rCO2})

at the end of the drainage stage are considered as an intrinsic property of CO_2-brine systems in sandstones. The viscous forces in CO_2-brine systems are very small due to the significant contrast between water and CO_2 viscosities (μ_{water}/μ_{CO2}≈11-58). In case of the absence of viscous forces and presence of high CO_2-water interfacial tension, the capillary pressure that is necessary to reach higher CO_2 saturation cannot be achieved resulting in very low end-point K_{rCO2}. Capillary end effect as discontinuity and holdup of the wetting phase at the core outlet may lead to serious errors in end-point relative permeability calculations. This phenomenon beside gravity segregation is also considered as experimental artefact that causes low end-point K_{rCO2} (Müller, 2011). Low K_{rCO2} and S_{CO2} cannot be counted as ultimate end-point values unless sufficient capillary pressure is achieved during the experiment (Krevor et al., 2012). The observed Kr_{CO2} in case of gaseous CO_2 is relatively lower than the supercritical CO_2 (Bennion and Bachu, 2005). The higher interfacial tension of gaseous CO_2 beside unfavorable lower magnitude of its viscosity results in more significant domination of the capillary over viscous forces and consequent lower K_{rCO2} (Benson et al., 2013; Li et al., 2012). Higher end-point K_{rCO2} and S_{CO2} for the low permeable but more homogeneous Basal Cambrian sandstone plug than the high permeable but more heterogeneous Viking sandstone was reported (Bennion and Bachu, 2005). The mentioned phenomenon was attributed to the lower degree of heterogeneity in case of tight sandstone core plug or lower contrast in pore size distribution that may result in the lower degree of bypassing of some portions of the pore space by the injected CO_2 and consequently higher end-point K_{rCO2}. A previous study (Falta et al., 2010) on two Berea sandstone core plugs by utilizing TOUGH2-ECO2N software illustrated that the heterogeneous core plug exhibits no significant correlation between the porosity and CO_2 saturation due to flow preference and permeability variations (Figure 11).

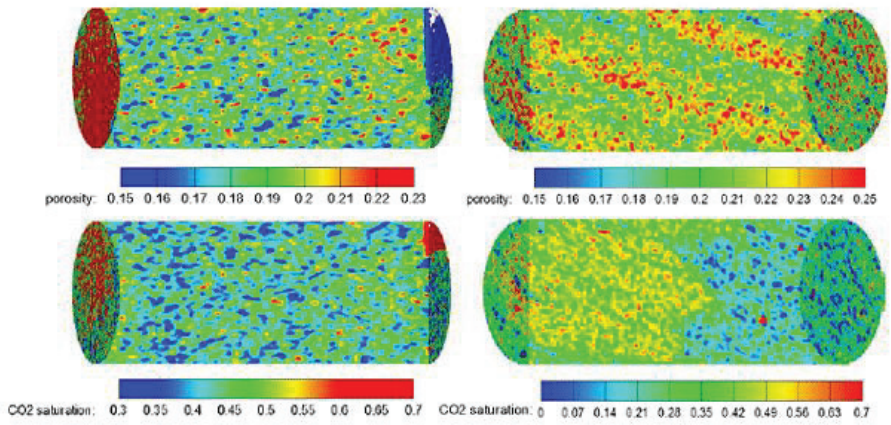

Figure 11: Effect of Heterogeneity on CO_2 distribution (Falta et al., 2010). Homogeneous (left) and the heterogeneous (right) cores

2.5.4. Residual CO_2 trapping

Due to the discontinuity of the CO_2 phase during the imbibition process, CO_2 will be trapped as immobile portion inside the water phase (Figure 3). Land trapping model (Land, 1968) is one of the most used models for modelling the residual trapped saturation of the CO_2 (S_{CO2t}) after adequate injected pore volumes of water during the imbibition process. This model is utilized to provide a relation between maximum saturation of the non-wetting phase at the end of the drainage process (S_{nwm}) and the trapped saturation of the non-wetting phase at the end of the imbibition process (S_{nwt}). In case of CO_2-water system the Land model (Land, 1968) becomes:

$$S_{CO2t} = \frac{S_{CO2m}}{1+C_L S_{CO2m}} \tag{22}$$

That can be rewritten as:

$$C_L = \frac{1}{S_{CO2t}} - \frac{1}{S_{CO2m}} \tag{23}$$

The Land's trapping coefficient (C_L) varies between [0-∞] in which C_L=0 corresponds the situation in which all the CO_2 is trapped while C_L=∞ represents the case of no CO_2 entrapment. Based on equation 18 dS_{CO2t}/dS_{CO2m}>0 that means that higher S_{CO2m} during the drainage cycle results in higher expected trapped CO_2 saturation (Figure 12).

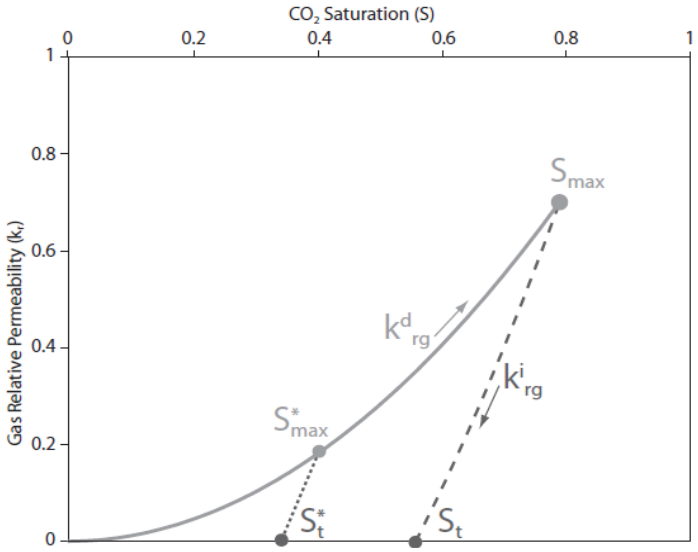

Figure 12: The dependency of the trapped CO_2 saturation (S_t) to the achieved CO_2 saturation (S_{max}) at the end of the drainage cycle (Burnside and Naylor, 2014)

Spiteri et al. (Spiteri et al., 2008) mentioned that for intermediate and mixed wet reservoirs, the residual CO_2 saturation does not increase uniformly by increasing the maximum achieved CO_2 saturation during the drainage process. They proposed a quadratic model for correlating the residual CO_2 saturation to the maximum achieved CO_2 saturation:

$$S_{CO2t} = \alpha S_{CO2m} - \beta S_{CO2m}^2 \quad (24)$$

In which α and β are fitting parameters that demonstrate the initial slop and the curvature of the considered relationship. Relative permeability hysteresis is the key phenomenon in entrapment of the injected CO_2 through residual trapping mechanism.

2.6. Implication on geomechanical integrity of cap rock

The injected CO_2 will be distributed laterally and vertically inside the saline aquifer and will move upward due to density difference and buoyancy effect. The upward migration of the injected CO_2 results in formation of gas cap beneath the surrounding cap rock that exerts mechanical stress to the cap rock. Although achieving the maximum possible CO_2 storage through utilizing the maximum porous portion of the target formation is an ideal plan, constrictions due to reaching the maximum formation pressure must be considered. Over-pressurization of the target aquifer due to injecting large amount of high pressure supercritical CO_2 may cause leakage into the surrounding environment breaching the geomechanical integrity of the sealing cap rock. The leakage can occur through reactivation of the existing faults, induced fractures inside the cap rock and through abandoned wells. Study by Juanes et al. (2006) revealed that relative permeability hysteresis in heterogeneous reservoir results in immobilization of some portion of the injected CO_2 plume during the imbibition process that prevents further upward migration of the CO_2 plume. The formation of high pressurized CO_2 gas cap beneath the cap rock is thus averted that could have put the integrity of the sealing cap rock at risk (Figure 13).

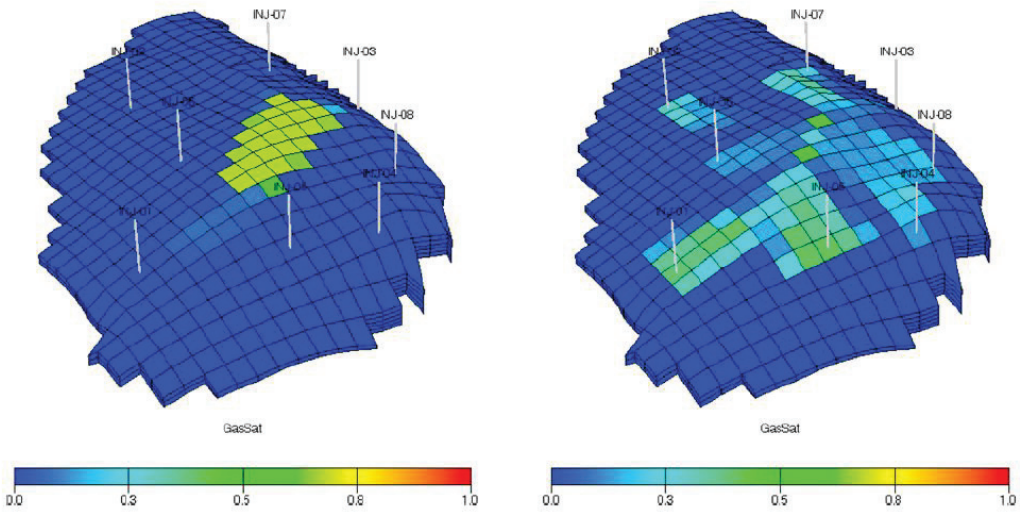

Figure 13: CO_2 distribution after 500 years in a reservoir without considering hysteresis (left) and with considering hysteresis (right) (Juanes et al., 2006)

3. Summary of the papers

The outcomes of this study that make the core of the PhD dissertation are three peer-reviewed journal papers that cover rock physical and fluid flow aspects of CO_2 storage in sandstone reservoirs. The first paper covers the rock physical behavior of CO_2 saturated sandstones and possibility of detecting CO_2 phase change by seismic monitoring in sandstone formations. The fluid flow and petrophysical aspects of CO_2 storage is covered in papers 2 and 3. Paper 2 is focused on permeability response of water and CO_2 saturated sandstones under varying P_p and σ_c conditions and their effective stress coefficient for the permeability. In paper 3 the relative permeability of CO_2-water systems in sandstones and its implication on CO_2 storage is extensively discussed.

3.1. Rock physical aspects of CO_2 storage and seismic monitoring

Paper I: 'Experimental investigation of seismic velocity behavior of CO_2 saturated sandstones under varying temperature and pressure conditions'. J. Naseryan Moghadam, N.H. Mondol, P. Aagaard and H. Hellevang 2016, Journal of Greenhouse Gases: Science and Technology, DOI: 10.1002/ghg.1603

3.1.1. Objectives

The main objective of this research task was to increase our understanding of impact of CO_2 phase transition on seismic velocities of CO_2 saturated sandstone. It was also aimed to investigate the role of sandstone porosity influencing seismic velocity changes due to CO_2 phase transition. Comparing the gas-liquid induced velocity change to the gas-supercritical state change was also a matter of interest for this study.

3.1.2. Materials and methodology

The utilized core plugs in this study were porous and permeable Red Wildmoor (Sherwood sandstone group, UK) and tight and low permeable Knorringfjellet (Longyearbyen, Svalbard, Norway) sandstones. The porosity contrast was used to investigate the dependency of the observed CO_2 induced velocity alteration to the rock porosity. The hydrostatic uniaxial cell

that was utilized for acoustic velocity measurement was equipped with radial and axial deformation sensors and seismic wave (V_p and V_s) receiving and transmitting transducers. The seismic velocities of sandstone core plugs were measured over an extensive range of temperature [22, 30 & 40°C] and pressure [1-17 MPa] to represent gaseous, liquid and supercritical states of CO_2.

3.1.3. Key findings

- Introducing CO_2 into both sandstone core plugs at all temperatures resulted in significant seismic velocity reduction up to the critical pressure due to increasing the density of the saturated samples and insignificant change of rock bulk modulus.
- The minimum velocities for both core plugs at each specific temperature were observed at the same interval that was predicted to be the CO_2 phase transition interval. This was regarded a clear indication of reaching phase boundary.
- The observed radial velocity reduction in case of Red Wildmoor core plug was in good agreement with the observed axial ones. The measured velocities in the recycle run for both core plugs demonstrated the same velocity reduction around the critical pressure for all three temperatures reflecting crossing the CO_2 dense state-gas boundary.
- The unchanged velocity behavior of water and N_2 saturated sandstones over the same temperature and pressure interval in which CO_2 saturated sandstones exhibits significant velocity alteration is attributed to CO_2 experiencing gas to dense-phase transition while the critical conditions for N_2 and H_2O is not achieved within the experiments.
- The observed axial velocity reduction compared to the dry state in case of highly porous Red Wildmoor sandstone ($\varphi \approx 27\%$) was slightly higher (ΔV_p=6% & ΔV_s=4%) than the low porosity Knorringfjellet ($\varphi \approx 11\%$) core plug (ΔV_p=4% & ΔV_s=2.6%). The observations proved a good correlation between the rock porosity and the observed velocity variation induced by CO_2 phase transition.
- Above critical pressure the observed V_p gradually increases for both core plugs due to increasing rock bulk modulus at higher pressure and almost constant density of the saturated rock. Due to independency of the V_s to fluid bulk modulus variation, the observed V_s above critical pressure remained unchanged.

- The observed velocity reduction at higher temperature (T=40°C) in which CO_2 gas to supercritical state transition occurs was smoother compared to lower temperature (T=22°C). This is due to the sharp contrast between physical properties of gaseous and liquid phases of CO_2 while there is a gradual change upon crossing the gaseous-supercritical boundary.
- These observations provide empirical confirmation for the possibility of detecting CO_2 phase transition by seismic monitoring technique under laboratory conditions for sandstones with wide range of porosities.
- Although due to the presence of irreducible in-situ pore fluids achieving the 100% CO_2 saturation is not possible inside the pore space, studying the seismic behavior of 100% CO_2 saturated sandstone can provide a reliable framework as an end member of CO_2 saturation. It can assist in better interpretation of seismic data for detecting CO_2 plume migration and possible CO_2 phase transition.

3.2. Fluid flow and petrophysical aspects of CO_2 storage in Sandstone reservoirs-Part I

Paper II: 'Effective stress law for the permeability of clay bearing sandstones by the Modified *Clay Shell Model*'. J. Naseryan Moghadam, N.H. Mondol, P. Aagaard and H. Hellevang 2016, Journal of Greenhouse Gases: Science and Technology, DOI: 10.1002/ghg.1612

3.2.1. Objectives

The main aim of this paper was to define the effective stress law by means of measuring the sensitivity of the sandstone permeability to the applied confining stress and pore pressures. Reducing the degree of complexity by stating the absolute permeability as a function of one parameter as effective stress instead of two parameters as P_p and σ_c by means of calculating the effective stress coefficient (α_k) was also desired. Better understanding the reservoir permeability alteration by CO_2 associated phenomena like pore pressure increase and effective stress reduction was also targeted. Investigating the impact of presence of highly compressible clay minerals in the pore structure and significant contrast between the elastic moduli of quartz and clay minerals on the resultant α_k was also a motive for pursuing this

study. It was also attempted to enhance the model-predicted α_k coefficients by modifying the current α_k models through considering spherical geometry.

3.2.2. Materials and methodology

The core plugs that were utilized in this study were Berea (Cleveland Quarries, Ohio, USA) and Knorringfjellet (Longyearbyen, Svalbard, Norway) sandstones. The considered sandstone core plugs were selected to investigate the impact of clay content contrast on the observed effective stress coefficient for the permeability. The CoreLab AFS-200 HP-HT flow rig was utilized to measure the absolute permeability of sandstone core plugs under varying confining stresses [6-17 MPa] while the utilized pore pressures [2, 3 and 4 MPa] were fixed. The measured permeability values were plotted versus the applied confining stresses and then by plotting the iso-perm lines, the correspondent pore pressures were plotted versus the applied confining stresses. α_k was calculated by measuring the slope of the mentioned cross-plots. The utilized test fluids were de-ionized water and CO_2 and the experiments were performed at room temperature (22 °C). In case of CO_2, the Klinkenberg correction was utilized to account for gas slippage effect.

3.2.3. Key findings

- The obtained permeability values for both sandstone core plugs were in good agreement with the previously reported values.
- The observed permeability values by utilizing water and CO_2 as test fluid demonstrated relatively low difference [<4%] for both core plugs. The higher CO_2 permeability is attributed to the gas slippage effect due to mean free path of the gas.
- The observed permeability values significantly decreased by increasing the applied confining stresses for both test fluids. The mentioned reduction followed closely a power law trend. It's due to the closure of the in-situ pores inside the porous medium.
- The observed permeability reduction at lower confining stresses is more significant. This phenomenon is due to rapid closure of low-aspect ratio cracks that are less resistant against the exerted confining stress. The lower permeability reduction at higher confining stresses is due to existence of high-aspect ratio pores that are resistant against further compaction.

- The absolute permeability of the Knorringfjellet core plug was more affected by confining stress as its smaller pore radius makes its flow capacity to be proportionally more affected compared to the more porous Berea core plug.
- Increase in pore pressure increased the observed permeability values. The compressible pore-filling kaolinite is subjected to the applied P_p due to its higher compressibility (lower elastic moduli) that results in increasing connected pore space and permeability.
- The proposed modified *Clay Shell Model* which considers spherical geometry has better performance in predicting the α_k values for both core plugs than previous proposed models. In this model the significant contrast between the compressibility of the quartz (solid framework) and pore space filling clay is considered the source of higher sensitivity of the rock permeability to the applied P_p and results in $\alpha_k>1$.
- The Calculated α_k values for the Berea [$1.18<\alpha_k<3.40$] were significantly higher than the Knorringfjellet [$1.24<\alpha_k<1.55$] core plug. This observation is believed to be in accordance with the higher percentage of kaolinite clay in Berea [4.76%] compared to the Knorringfjellet [0.6%] core plug.
- The increasing trend of α_k by increasing σ_c is attributed to the lower sensitivity of rock permeability to the applied σ_c compared to P_p at higher σ_c that results in stronger resistance of the rock against further compaction and permeability alteration. The α_k =2.6 and α_k =1.38 can be regarded as an average value for Berea and Knorringfjellet sandstones respectively that are in good agreement with previously reported values.
- Application of Terzaghi effective stress law or assuming $\alpha_k\approx1$ in case of low porous rock with relatively low amount of clay is justifiable.
- The proposed spherical geometry is capable of providing more realistic α_k estimation by considering moderate to low elastic moduli for clay minerals while the previous models require extremely low elastic moduli values for a proper α_k estimation. Application of the moderate elastic moduli by previous models results in under-estimation of α_k values.
- The presented correlation for stating the α_k as a function of the applied P_p and σ_c is capable of estimating α_k for the given stress interval.

3.3. Fluid flow and petrophysical aspects of CO_2 storage in Sandstone reservoirs- Part II

Paper III: 'Determination of CO_2-Brine relative permeability curves for the low permeable Knorringfjellet (Svalbard, Norway) and permeable Berea sandstones'. J. Naseryan Moghadam, N.H. Mondol, P. Aagaard and H. Hellevang, submitted to International Journal of Greenhouse Gas Control on 9 September 2016 (under review)

3.3.1. Objectives

The aim of this study was to experimentally determine the drainage and imbibition relative permeability curves for the Knorringfjellet and Berea sandstones. The Knorringfjellet sandstone was targeted as it has been recently considered as potential for a pilot CO_2 storage project. The selected sandstone samples represent a wide range of petrophysical properties like porosity, permeability, clay content and wettability. In-detail analyzing the hysteresis phenomenon due to the existence of multiple interstitial fluid distributions for each level of saturation and its impact on residual trapping of CO_2 was also aimed. Observation of relative permeability behavior of gaseous CO_2-water system instead of supercritical CO_2 was an additional motive for pursuing this research. The impact of petrophysical parameters like heterogeneity and rock wettability on the extent of the observed CO_2 relative permeability was also analyzed. Better understanding of the lower amount of the observed CO_2 end-point relative permeability was also aimed.

3.3.2. Materials and methodology

The utilized core plugs in this study were Knorringfjellet (Longyearbyen, Svalbard, Norway) and Berea (Cleveland Quarries, Ohio, USA) sandstones. The *unsteady state* relative permeability measurement method was utilized to determine the drainage and imbibition relative permeability curves for two sandstone core plug. The porosity of the samples was determined by measuring the difference between the weight of dry and water saturated samples. The experiments were performed by utilizing the CoreLab AFS-200 HP-HT flow system and applying constant confining pressure [P_c=8 MPa] and back pressure [P_{out}=3 MPa] for maintaining gaseous CO_2 condition. During the drainage cycle, applied constant CO_2 flow rates were 0.5 and 0.1cm^3/min for the Berea and Knorringfjellet core plugs respectively. The considered flow rates during the water injection (imbibition) for the Knorringfjellet core plug

was lower [0.05 cm^3/min] to account for its low permeability and preventing pressure buildup at the core inlet. In-situ saturation of the fluids was measured by taking out the sample after fulfilling each displacement stage.

3.3.3. Key findings

- The observed end-point CO_2 saturation ($0.40<S_{CO2m}<0.44$) and relative permeability ($0.13<K_{rCO2}<0.18$) after finalizing the drainage cycle were relatively low. This observation was in good agreement with the previous reports in which the relative permeability of the CO_2-water systems in sandstones was studied.
- This phenomenon is believed to be an intrinsic property of CO_2-water systems and is attributed to very low CO_2 viscosity and domination of capillary forces over viscous forces that inhibits effective sweeping of the in-situ water and achieving higher CO_2 saturation and relative permeability.
- Relatively high CO_2 fractional flow was observed at relatively high residual saturations of in-situ water ($0.56<S_{wi}<0.60$) after drainage cycle. The Brook-Corey and modified Pirson's correlations could successfully simulate the fractional flow and the relative permeability curves for CO_2-water system in sandstone core plugs.
- In case of lack of experimental equipment, the capillary pressure curves for CO_2-water systems were successfully estimated by utilizing Brook-Corey and Kwon-Pickett correlations and utilizing saturation, porosity and relative permeability data. The obtained P_c data are in good agreement with previous studies.
- Due to the unfavorable lower viscosity and higher interfacial tension in case of gaseous CO_2, the obtained CO_2 relative permeability data were slightly lower than the reported values in which the supercritical CO_2 were utilized.
- Higher heterogeneity due to the higher degree of contrast in pore size distribution might lead to higher degree of bypassing of some portion of the pore space by CO_2. The mentioned phenomenon may lead to lower K_{rCO2} in case of higher permeable but heterogeneous sandstone compared to lower permeable but homogenous sandstone.
- Although the CO_2-water systems in sandstones are characterized to be water-wet, presence of hydrophobic kaolinite and hydrophilic smectite may affect the wettability of the system toward CO_2. Strong decrease in K_{rw} by introducing CO_2 into the system is also considered as an indication for water wettability of CO_2-water systems.

- The snap-off phenomenon in water-wet systems in which CO_2 discontinuity, in the form of trapped CO_2 bubbles, occurs in larger pores, and is considered as the deriving mechanism for CO_2 trapping in imbibition cycle. The higher achieved CO_2 saturation during drainage cycle results in higher trapped CO_2 saturation during imbibition cycle that can be justified by the Land trapping model.
- A relatively large magnitude of the injected CO_2 can be immobilized inside the pore space ($0.20<S_{CO2t}<0.24$) due to the hysteresis phenomenon after the first drainage-imbibition cycle. This provides an empirical confirmation for the significant role of CO_2 residual trapping mechanism, especially at the early stages of the CO_2 storage operation.

4. Concluding remarks & future study

The main contribution and conclusion of this thesis is summarized as:

4.1. Rock physics experiments:

- The performed rock physics experiments on the sandstone core plugs revealed that the seismic response of the CO_2 saturated sandstone is significantly affected by the current thermodynamical state of the CO_2 inside the pore space. This phenomenon is observed as abrupt change in acoustic velocities (V_p and V_s) at lower temperature (T=22°C) and smooth change at higher temperature (T=40°C). The observed behavior is attributed to crossing CO_2 gas-liquid boundary conditions at lower temperatures and existence of significant contrast between the physical properties of gaseous and liquid states of the CO_2. Supercritical CO_2 is preferred for CO_2 sequestration purposes due to its higher density. The required temperature and pressure conditions for CO_2 gas-dense phase transition are achievable within the uppermost kilometer of the sedimentary basin. The performed experiments revealed that the CO_2 phase transition that may affect the mobility of the injected CO_2 plume can be detected under the laboratory conditions by means of seismic monitoring. Even though achieving 100% CO_2 saturation in real conditions is not possible, the performed experiments provide data of a fully CO_2 saturation end member that can be useful in better interpretation of seismic monitoring.

4.2. Fluid flow and petrophysical experiments:

- The performed fluid flow experiments demonstrated that the absolute permeability of the sandstone core plugs was greatly influenced by the applied confining stresses and pore pressures. While clays (either coating or pore filling) were exposed to the applied pore pressure, the exerted confining stress was solely supported by the quartz matrix. Due to the higher compressibility of the clay minerals compared to the quartz, the sensitivity of the sandstone permeability to applied pore pressure was higher than that of applied confining stress. This leads to higher α_k coefficient. The performed experiments revealed the same permeability behavior in both cases of water and CO_2

as test fluids. The proposed *Modified Clay Shell model* with spherical geometry was capable of estimating higher α_k values that were closer to the observed values. The experiments revealed that permeability enhancement is expected in case of increasing CO_2 pressure regardless of the considered confining stress that can be a matter of interest for CO_2 sequestration purposes.

- The performed relative permeability experiments revealed very low CO_2 end-point relative permeability values and water wettability characteristics in case of CO_2-water systems in saline aquifers. The very low K_{rCO2} is described to be due to domination of the capillary forces over viscous forces in case of CO_2-water systems. In case of gaseous CO_2, the observed K_{rCO2} is even lower due to its unfavorable lower viscosity and higher interfacial tension that leads to less effective sweeping the in-situ water and preventing to achieve higher CO_2 saturations. Pore space heterogeneity plays a crucial role in determining the maximum CO_2 saturation as significant contrast in pore size distribution may cause bypassing of some portion of the pore space and consequent low CO_2 saturation. The residual trapping due to the permeability hysteresis is demonstrated to be a significant storage mechanism as a great portion of the injected CO_2 can be immobilized inside the pore space at the early stages of CO_2 sequestration program. The mentioned phenomenon in the heterogeneous storage medium may trap a significant quantity of the injected CO_2. It prevents lateral and/or upward migration and formation of the CO_2 plume beneath the sealing cap rock that might put the geomechanical integrity of the cap rock at risk.

4.3. Future research within the study area:

- Studying seismic response of saturated sandstone samples with varying S_{CO2}/S_{water} ratio at different temperatures and pressures is highly recommended to account for the possibility of CO_2 state transition detection in real reservoir conditions in which multiple in-situ pore fluids are present. Measurement of resistivity response of the mentioned core plugs might also provide a reliable tool for monitoring the CO_2 plume migration inside the reservoir and detecting any possible phase transition and CO_2 leakage.

- Analyzing the role of the anisotropy on the observed effective stress coefficient for the permeability by performing permeability measurements on sandstone core plugs that are cut from the same core block but with different cutting angles is strongly recommended. Quantifying the impact of clay content on the observed α_k coefficients by performing permeability measurement on both synthetic and reservoir core plugs with varying clay content under varying confining stress and pore pressure conditions can also be considered.

- Due to the limitation of the system for measuring very low pressure differences (1-10 Pa) along the core specially in case of very high permeable core samples (K_a>200 mD), it is recommended to equip the flooding system with gauge and differential pressure transducers with higher degree of precision. It assists in further improvement of the fluid displacement experiments by achieving higher quality/more reliable data and better understanding the topic.

- Precise measurement of fluid saturation inside the core during displacement experiments has a crucial role in relative permeability calculation. In order to improve the degree of precision of saturation measurement, in-situ measurement of the fluid saturation inside the core by means of computed tomography (CT) imaging through utilizing more advanced flooding systems like CoreLab AXRP-300 (Automated X-Ray Relative Permeability System) is recommended.

- Performing the reservoir simulation by conventional reservoir simulators like CMG and ECLIPSE by means of utilizing the observed relative permeability data can provide a powerful insight about the significant role of the relative permeability hysteresis on the residual CO_2 trapping mechanism. Analyzing the CO_2 trapping response of the sandstones under successive drainage-imbibition cycles and interpreting the observations by the available trapping models can also be considered suitable for following up the current research.

5. References

Abaci, S., Edwards, J.S., Whittaker, B.N., 1992. Relative permeability measurements for two phase flow in unconsolidated sands. Mine Water and the Environment 11, 11-26.

Abdallah, W., Buckley, J.S., Carnegie, A., Edwards, J., Herold, B., Fordham, E., Graue, A., Habashy, T., Seleznev, N., Signer, C., 1986. Fundamentals of wettability. Technology 38, 1125-1144.

Ahmed, T., 2010a. Chapter 4 - Fundamentals of Rock Properties, in: Ahmed, T. (Ed.), Reservoir Engineering Handbook (Fourth Edition). Gulf Professional Publishing, Boston, p. 1472.

Ahmed, T., 2010b. Chapter 5 - Relative Permeability Concepts, in: Ahmed, T. (Ed.), Reservoir Engineering Handbook (Fourth Edition). Gulf Professional Publishing, Boston, p. 1472.

Al-Wardy, W., Zimmerman, R.W., 2004. Effective stress law for the permeability of clay-rich sandstones. Journal of Geophysical Research: Solid Earth 109, 1-10.

Amyx, J.W., Bass, D.M., Whiting, R.L., 1960. Petroleum Reservoir Engineering: Physical properties. McGraw-Hill, p. 610.

Arts, R., Eiken, O., Chadwick, A., Zweigel, P., van der Meer, B., Kirby, G., 2004. Seismic monitoring at the Sleipner underground CO2 storage site (North Sea). Geological Society, London, Special Publications 233, 181-191.

Arts, R., Winthaegen, P., 2005. Monitoring Options for CO2 Storage. 2, 1001-1013.

Avseth, P., Mukerji, T., Mavko, G., 2010. Quantitative Seismic Interpretation: Applying Rock Physics Tools to Reduce Interpretation Risk. Cambridge University Press, p. 408.

Bachu, S., 2000. Sequestration of CO2 in geological media: criteria and approach for site selection in response to climate change. Energy Conversion and Management 41, 953-970.

Bachu, S., Bonijoly, D., Bradshaw, J., Burruss, R., Holloway, S., Christensen, N.P., Mathiassen, O.M., 2007. CO2 storage capacity estimation: Methodology and gaps. International Journal of Greenhouse Gas Control 1, 430-443.

Batzle, M.L., Wang, Z., 1992. Seismic properties of pore fluids. Geophysics 57, 1396-1408.

Beaubien, S.E., Lombardi, S., Ciotoli, G., Annuziatellis, A., Hatziyannis, G., Metaxas, A., Pearce, J.M., 2005. Potential hazards of CO2 leakage in storage systems—Learning from natural systems, Greenhouse Gas Control Technologies 7. Elsevier Science Ltd, Oxford, pp. 551-560.

Bennion, B., Bachu, S., 2005. Relative Permeability Characteristics for Supercritical CO2 Displacing Water in a Variety of Potential Sequestration Zones, SPE Annual Technical Conference and Exhibition. Society of Petroleum Engineers, Dallas, Texas.

Benson, S.M., Cook, P., Anderson, J., Bachu, S., Nimir, H.B., Basu, B., Bradshaw, J., Deguchi, G., Gale, J., Goerne, G.v., Heidug, W., Holloway, S., Kamal, R., Keith, D., Lloyd, P., Rocha, P., Senior, B., Thomson, J., Torp, T., Wildenborg, T., 2005. Special report on carbon dioxide capture and storage, Intergovernmental panel on climate change (IPCC), p. 431.

Benson, S.M., Pini, R., Reynolds, C., Krevor, S., 2013. Relative permeability analysis to describe multi-phase flow in CO2 storage reservoirs. Global CCS Institute, p. 51.

Bernabe, Y., 1986. The effective pressure law for permeability in Chelmsford granite and Barre granite. International Journal of Rock Mechanics and Mining Sciences & Geomechanics Abstracts 23, 267-275.

Bernabe, Y., 1987. The effective pressure law for permeability during pore pressure and confining pressure cycling of several crystalline rocks. Journal of Geophysical Research: Solid Earth 92, 649-657.

Berryman, J.G., 1992. Effective stress for transport properties of inhomogeneous porous rock. Journal of Geophysical Research: Solid Earth 97, 17409-17424.

Berryman, J.G., 1993. Effective-stress rules for pore-fluid transport in rocks containing two minerals. International Journal of Rock Mechanics and Mining Sciences & Geomechanics Abstracts 30, 1165-1168.

Bjørlykke, K., Mo, A., Palm, E., 1988. Modelling of thermal convection in sedimentary basins and its relevance to diagenetic reactions. Marine and Petroleum Geology 5, 338-351.

Brace, W.F., 1978. A note on permeability changes in geologic material due to stress. Journal of Pure and Applied Geophysics 116, 627-633.

Burnside, N.M., Naylor, M., 2014. Review and implications of relative permeability of CO2/brine systems and residual trapping of CO2. International Journal of Greenhouse Gas Control 23, 1-11.
Busch, A., Amann-Hildenbrand, A., 2013. Predicting capillarity of mudrocks. Marine and Petroleum Geology 45, 208-223.
Chadwick, A., Williams, G., Delepine, N., Clochard, V., Labat, K., Sturton, S., Buddensiek, M.-L., Dillen, M., Nickel, M., Lima, A.L., Arts, R., Neele, F., Rossi, G., 2010. Quantitative analysis of time-lapse seismic monitoring data at the Sleipner CO2 storage operation. The Leading Edge 29, 170-177.
Chen, C., Zeng, L., Shi, L., 2013. Continuum-scale convective mixing in geological CO2 sequestration in anisotropic and heterogeneous saline aquifers. Advances in Water Resources 53, 175-187.
Chowdhury, M., Schmitt, D.R., 2013. Seismic behaviour of CO2 saturated Fontainebleau sandstone under in situ conditions, Integration. GeoConvention, Calgary, pp. 1-7.
CO2-Capture-Project, 2015. CCP. Phase Four Participating Organizations, http://www.co2captureproject.org/.
Cook, P.J., 1999. Sustainability and Nonrenewable Resources. Environmental Geosciences 6, 185-190.
Dake, L.P., 1983. Fundamentals of Reservoir Engineering, Developments in Petroleum Science Elsevier Science, Netherlands, p. 437.
Darcy, H., 1856. Les Fontaines Publiques de la Ville de Dijon,, Dalmont, Paris, p. 647.
Darcy, H., 1857. Recherches Experimentales Relatives au Mouvement de l'Eau dans les Tuyaux. Mallet-Bachelier, Paris, p. 268.
Falta, R.W., Benson, S.M., Murdoch, L.C., 2010. Understanding and Managing Risks Posed by Brines Containing Dissolved Carbon Dioxide. United States Environmental Protection Agency (EPA), https://cfpub.epa.gov.
Farokhpoor, R., Lindeberg, E.G.B., Mørk, M.B.E., Torsæter, O., Mørk, A., 2012. CO2-Brine Relative Permeability Characteristics of Low Permeable Sandstones in Svalbard, International Symposium-Society of Core Analysts, Aberdeen, Scotland.
Firoozabadi, A., Cheng, P., 2010. Prospects for subsurface CO2 sequestration. AIChE Journal 56, 1398-1405.
Gassmann, F., 1951. Elasticity of porous media: Uber die Elastizitat poroser Medien, Vierteljahrsschrift der Naturforschenden Gesselschaft Zurich pp. 1-23.
Gray, D.H., Fatt, I., 1963. The effect of stress on permeability of Sandstone cores. Society of Petroleum Engineers Journal 3, 95-100.
Gutierrez, M., Katsuki, D., Almrabat, A., 2012. Effects of CO2 injection on the seismic velocity of sandstone saturated with saline water. International Journal of Geosciences 3, 908-917.
Hellevang, H., 2015. Carbon Capture and Storage (CCS), in: Bjørlykke, K. (Ed.), Petroleum Geoscience: From Sedimentary Environments to Rock Physics. Springer Berlin Heidelberg, Berlin, Heidelberg, pp. 591-602.
Hellevang, H., Pham, V.T.H., Aagaard, P., 2013. Kinetic modelling of CO2–water–rock interactions. International Journal of Greenhouse Gas Control 15, 3-15.
Honarpour, M., Mahmood, S.M., 1988. Relative-Permeability Measurements: An Overview. 40, 963 - 966.
Hunter, L., 2010. CO2 flow measurement key in CCS schemes, After Tuvnel.com. Power Engineering International (Pei) print publication, http://www.powerengineeringint.com/articles/print/volume-18/issue-4/features/co2-flow-measurement-key-in-ccs-schemes.html.
IEA, 2015. CO2 Emissions From Fuel Combustion Highlights 2015. International Energy Agency (IEA), 136.
Iglauer, S., 2011. Dissolution trapping of carbon dioxide in reservoir formation brine-a carbon storage mechanism. INTECH Open Access Publisher, p. 824.
Johnson, E.F., Bossler, D.P., Bossler, V.O.N., 1959. Calculation of Relative Permeability from Displacement Experiments. SPE-1023-G 216, 370-372.
Juanes, R., Spiteri, E.J., Orr, F.M., Blunt, M.J., 2006. Impact of relative permeability hysteresis on geological CO2 storage. Water Resources Research 42, 1-13.
Kiepe, J., Horstmann, S., Fischer, K., Gmehling, J., 2002. Experimental determination and prediction of gas solubility data for CO2+ H2O mixtures containing NaCl or KCl at temperatures between 313 and 393 K and pressures up to 10 MPa. Industrial & engineering chemistry research 41, 4393-4398.

Klinkenberg, L.J., 1941. The permeability of porous media to liquids and gases, Drilling and Production Practice. American Petroleum Institute, pp. 200-213.
Krevor, S.C.M., Pini, R., Zuo, L., Benson, S.M., 2012. Relative permeability and trapping of CO_2 and water in sandstone rocks at reservoir conditions. Water Resources Research 48, 16.
Land, C.S., 1968. Calculation of imbibition relative permeability for two-and three-phase flow from rock properties. Society of Petroleum Engineers Journal 8, 149-156.
Lazaratos, S.K., Marion, B.P., 1997. Crosswell seismic imaging of reservoir changes caused by CO2 injection. The Leading Edge 16, 1300-1308.
Leitner, W., 2000. Green chemistry: Designed to dissolve. Nature 405, 129-130.
Lemmon, E.W., McLinden, M.O., Friend, D.G., In: Linstrom, P.J., Mallard, W.G., 2011. Thermophysical properties of fluid systems in NIST chemistry webBook, NIST Standard Reference Database Number 69, National Institute of Standards and Technology, http://webbook.nist.gov.
Li, X., Boek, E.S., Maitland, G.C., Trusler, J.P.M., 2012. Interfacial Tension of (Brines + CO2): CaCl2(aq), MgCl2(aq), and Na2SO4(aq) at Temperatures between (343 and 423) K, Pressures between (2 and 50) MPa, and Molalities of (0.5 to 5) mol·kg–1. Journal of Chemical & Engineering Data 57, 1369-1375.
Mavko, G., Mukerji, T., Dvorkin, J., 2009. The Rock Physics Handbook, 2 ed. Cambridge University Press, Cambridge, UK, p. 524.
Mondol, N.H., Jahren, J., Bjørlykke, K., Brevik, I., 2008. Elastic properties of clay minerals. The Leading Edge 27, 758-770.
Mukerji, T., Mavko, G., 1994. Pore fluid effects on seismic velocity in anisotropic rocks. Geophysics 59, 233-244.
Müller, N., 2011. Supercritical CO2-Brine Relative Permeability Experiments in Reservoir Rocks—Literature Review and Recommendations. Transp Porous Med 87, 367-383.
Mørk, M.B.E., 2013. Diagenesis and quartz cement distribution of low-permeability Upper Triassic–Middle Jurassic reservoir sandstones, Longyearbyen CO_2 lab well site in Svalbard, Norway. AAPG Bulletin 97, 577-596.
Naseryan Moghadam, J., Mondol, N.H., Aagaard, P., Hellevang, H., 2016. Effective stress law for the permeability of clay-bearing sandstones by the Modified Clay Shell model. Greenhouse Gases: Science and Technology, DOI: 10.1002/ghg.1612.
Njiekak, G., Schmitt, D.R., Yam, H., Kofman, R.S., 2013. CO2 rock physics as part of the Weyburn-Midale geological storage project. International Journal of Greenhouse Gas Control 16, 118-133.
Njobuenwu, D., O,., Oboho, E., O,., H., R., 2007. Determination of Contact Angle from Contact Area of Liquid Droplet Spreading on Solid Substrate. Leonardo Electronic Journal of Practices and Technologies 6, 29-38.
Oak, M.J., Baker, L.E., Thomas, D.C., 1990. Three-phase relative permeability of Berea Sandstone. Journal of Petroleum Technology 42, 1054-1061.
Pentland, C.H., El-Maghraby, R., Georgiadis, A., Iglauer, S., Blunt, M.J., 2011. Immiscible Displacements and Capillary Trapping in CO2 Storage. Energy Procedia 4, 4969-4976.
Riaz, A., Hesse, M., Tchelepi, H., Orr, F., 2006. Onset of convection in a gravitationally unstable diffusive boundary layer in porous media. Journal of Fluid Mechanics 548, 87-111.
Ringrose, P.S., Mathieson, A.S., Wright, I.W., Selama, F., Hansen, O., Bissell, R., Saoula, N., Midgley, J., 2013. The In Salah CO2 Storage Project: Lessons Learned and Knowledge Transfer. Energy Procedia 37, 6226-6236.
Ruprecht, C., Pini, R., Falta, R., Benson, S., Murdoch, L., 2014. Hysteretic trapping and relative permeability of CO2 in sandstone at reservoir conditions. International Journal of Greenhouse Gas Control 27, 15-27.
Rutqvist, J., Birkholzer, J., Cappa, F., Tsang, C.F., 2007. Estimating maximum sustainable injection pressure during geological sequestration of CO2 using coupled fluid flow and geomechanical fault-slip analysis. Energy Conversion and Management 48, 1798-1807.
Shi, J.Q., Xue, Z., Durucan, S., 2007. Seismic monitoring and modelling of supercritical CO2 injection into a water-saturated sandstone: Interpretation of P-wave velocity data. International Journal of Greenhouse Gas Control 1, 473-480.
Sifuentes, W.F., Giddins, M.A., Blunt, M.J., 2009. Modeling CO2 Storage in Aquifers : Assessing the key contributors to uncertainty, Offshore Europe. Society of Petroleum Engineers, Aberdeen, UK.

Skov, T., Borgos, H.G., Halvorsen, K., Å.,, Randen, T., Sønneland, L., Arts, R., Chadwick, A., 2002. Monitoring And Characterization of a CO2 Storage Site. Society of Exploration Geophysicists, pp. 1669-1672.
Spiteri, E.J., Juanes, R., Blunt, M.J., Orr, F.M., 2008. A New Model of Trapping and Relative Permeability Hysteresis for All Wettability Characteristics. SPE Journal 13, 277 - 288.
Streit, J.E., Hillis, R.R., 2004. Estimating fault stability and sustainable fluid pressures for underground storage of CO2 in porous rock. Energy 29, 1445-1456.
Thomas, R.D., Ward, D.C., 1972. Effect of Overburden Pressure and Water Saturation on Gas Permeability of Tight Sandstone Cores. Journal of Petroleum Technology 24, 120-124.
Walls, J., Nur, A., 1979. pore pressure and confining pressure dependence of permeability in sandstone, Seventh formation evaluation symposium of the Canadian Well Logging Society, Calgary.
Walsh, J.B., 1981. Effect of pore pressure and confining pressure on fracture permeability. International Journal of Rock Mechanics and Mining Sciences & Geomechanics Abstracts 18, 429-435.
Wang, Z., Cates, M.E., Langan, R.T., 1998. Seismic monitoring of a CO2 flood in a carbonate reservoir: A rock physics study. Geophysics 63, 1604-1617.
Wang, Z., Nur, A.M., 1989. Effects of CO2 Flooding on Wave Velocities in Rocks With Hydrocarbons. SPE Reservoir Engineering 4(4), 429-436.
Welge, H.J., 1952. A Simplified Method for Computing Oil Recovery by Gas or Water Drive. Journal of Petroleum Technology 4, 91-98.
White, D., 2009. Monitoring CO2 storage during EOR at the Weyburn-Midale Field. The Leading Edge 28, 838-842.
Woeber, A.F., Katz, S., Ahrens, T.J., 1963. Elasticity of selected rocks and minerals. Geophysics 28, 658-663.
Wyble, D.O., 1958. Effect of Applied Pressure on the Conductivity, Porosity and Permeability of Sandstones. Journal of Petroleum Technology 10, 57-59.
Yam, H., Schmitt, D., 2011. CO2 Rock Physics: A laboratory study, Recovery 2011; CSPG CSEG CWLS Convention.
Zhang, D., Song, J., 2014. Mechanisms for Geological Carbon Sequestration. Procedia IUTAM 10, 319-327.
Zoback, M.D., Byerlee, J.D., 1975. Permeability and Effective Stress. AAPG Bulletin 59, 154-158.

Paper I

Experimental investigation of seismic velocity behavior of CO_2 saturated sandstones under varying temperature and pressure conditions

By:

Javad Naseryan Moghadam, Nazmul Haque Mondol,
Per Aagaard and Helge Hellevang

Journal of Greenhouse Gases: Science and Technology
(DOI: 10.1002/ghg.1603)

Paper II

Effective stress law for the permeability of clay bearing sandstones by the Modified Clay Shell Model

By:

Javad Naseryan Moghadam, Nazmul Haque Mondol,
Per Aagaard and Helge Hellevang

Journal of Greenhouse Gases: Science and Technology
(DOI: 10.1002/ghg.1612)

Paper III

Determination of CO2-Brine relative permeability curves for the tight Knorringfjellet (Svalbard, Norway) and permeable Berea sandstones

By:

Javad Naseryan Moghadam, Nazmul Haque Mondol,
Per Aagaard and Helge Hellevang

International Journal of Greenhouse Gas Control
(Submitted-under review)

Appendix

Extended Abstract I

Evaluation of mechanical strength of a Barents Sea Shale by applying the most common failure criteria

By:

Javad Naseryan Moghadam,
Nazmul Haque Mondol, and Per Aagaard

Third EAGE Shale Workshop on Shale Physics and Shale Chemistry: New Plays, New Science, New Possibilities, 23-25 January 2012, Barcelona, Spain
(DOI: 10.3997/2214-4609.20143917)

EAGE
EUROPEAN ASSOCIATION OF GEOSCIENTISTS & ENGINEERS

Evaluation of Mechanical Strength of a Barents Sea Shale by Applying the Most Common Failure Criteria

J. Naseryan Moghadam* (University of Oslo), N.H. Mondol* (University of Oslo / Norwegian Geotechnical Institute) and P. Aagaard* (University of Oslo)

SUMMARY

One of the important factors in formation of a petroleum reservoir and also a successful CO_2 storage operation is an efficient seal that prevents migration of accumulated hydrocarbon or injected CO_2 to the surrounding environments. In siliciclastic environment, shales and mudrocks are most common seals that prevent migration of hydrocarbon and CO_2 from reservoirs. This study investigates the most common failure criteria (Mohr-Coulomb Criterion, Drucker-Prager Criterion, Mogi Empirical Criterion and Hoek and Brown Criterion) by using a triaxial data set. The maximum effective principal stress (σ_1), one of the most important mechanical properties of caprocks that has crucial importance in rock strength calculations, has been predicted with the mentioned failure criteria. The applied data are obtained from a range of triaxial tests that were performed on a Barents Sea Shale cored from the Hekkingen Formation in two depth intervals. Among the applied failure criteria, Mogi failure criterion had the best performance in predicting the σ_1 of the tested shales, while the traditional Mohr-Coulomb criterion showed good prediction compared to complicated calculations suggested by other criteria. Also the observed considerable discrepancies between the obtained mechanical parameters for horizontal and vertical samples at same depth reveals the anisotropy in the Hekkingen Formation.

Introduction

Caprock seals are formations that prevent the migration of hydrocarbon and storage CO_2 to the surrounding formations. Shales and mudstones are most abundant formations in the sedimentary basin that can be found as caprock seals because of their low permeabilities. The most important mechanical parameter of the caprocks is the main principal stress that has crucial importance in exact determination of rock strength, fracture calculations and failure criteria. In this study, the most common failure criteria have been applied to analyze the triaxial test data that are obtained from geomechanical tests performed on the Hekkingen shales from the Barents Sea. The Hekkingen Formation consists of brownish-grey to very dark grey shale and claystone with occasional thin interbeds of limestone, dolomite, siltstone and sandstone. The core samples belonging to the Hekkingen Formation are selected from two depth intervals and are named as G_1 and G_2 (Table 1).

Materials and Methods

The most common failure criteria used in this study to evaluate mechanical strength of Hekkingen shales are Mohr-Coulomb Criterion (MC), Drucker-Prager Criterion (DP), Mogi Empirical Criterion (MEC) and Hoek and Brown Criterion (HB). Brief descriptions of the most common failure criteria are given bellow:

Mohr-Coulomb Criterion (1900 & 1976): Coulomb (1976) introduced the simplest and most important failure criterion for rock. He suggested that rock failure in compression takes place when the shear stress (τ) that is developed on a specific plane reaches a value that is sufficient to overcome both the natural cohesion of the rock plus the frictional force that opposes motion along the failure plane. The criterion can be written as

$$\tau = c + \sigma_n \tan(\varphi) \quad (1)$$

where σ_n is the normal stress acting on the failure plane, c is the cohesion of the material and φ is the angle of internal friction (Fjær et al., 1992). Mohr (1900) suggested that at failure, the normal and shear stresses across the failure plane are related by

$$\tau = f(\sigma_n) \quad (2)$$

where f is some function that is assumed to be obtained experimentally. A linear form of Mohr's criterion is equivalent to the Coulomb criterion. Consequently, a linear failure criterion such as Eq. (1) is often known as the Mohr–Coulomb criterion. There are two major components of this criterion. The first is the assumption that, at failure, the major principal stress (σ_1) is a linearly increasing function of the minor principal stress (σ_3). The second aspect of this criterion is the assumption that the value of the intermediate principal stress (σ_2) has no influence on the rock strength (Fjær et al., 1992).

Drucker-Prager Criterion (1952): The criterion was introduced to deal with the plastic deformation of soils and later applied to rocks. The DP criterion has defined a yield function for failure criterion as:

$$J_2^{\frac{1}{2}} = k + \alpha J_1 \quad (3)$$

where α and k are material constants, J_1 is the mean effective confining stress and J_2 is the deviatoric stress defined as:

$$J_1 = \frac{\sigma_1 + \sigma_2 + \sigma_3}{3} \quad (4) \qquad J_2^{1/2} = \sqrt{\frac{1}{6}((\sigma_1 - \sigma_2)^2 + (\sigma_1 - \sigma_3)^2 + (\sigma_2 - \sigma_3)^2)} \quad (5)$$

$$J_2^{\frac{1}{2}} = \left(\frac{3}{2}\right)^{\frac{1}{2}} \tau_{oct} \quad (6) \qquad \tau_{oct} = \frac{1}{3}\sqrt{((\sigma_1 - \sigma_2)^2 + (\sigma_1 - \sigma_3)^2 + (\sigma_2 - \sigma_3)^2)} \quad (7)$$

τ_{oct} and σ_2 are the octahedral shear stress and the mean effective principal stress respectively. The Coefficients in the outer bound (Circumscribed) Drucker-Prager criterion (CDP) and the inner bound (Inscribed) Drucker-Prager criterion (IDP)are (McLean and Addis, 1990):

$$\alpha_{CDP} = \frac{\sqrt{3}(q-1)}{q+2} \quad (8) \qquad k_{CDP} = \frac{\sqrt{3}C_0}{q+2} \quad (9)$$

$$\alpha_{IDP} = \frac{3Sin\varphi}{\sqrt{9 + 3Sin^2\varphi}} \quad (10) \qquad k_{IDP} = \frac{3C_0 Cos\varphi}{2\sqrt{q(9 + 3Sin^2\varphi)}} \quad (11)$$

Mogi Empirical Criterion (1971): Mogi failure criterion considered the influence of the intermediate principal stress (σ_2) on rock failure. He conducted the first extensive polyaxial compressive tests in rocks and noted that the intermediate principal stress does indeed have an impact on rock strength, and that brittle fracture occurs along a plane striking in the σ_2 direction. Mogi suggested a new failure criterion expressed as

$$\tau_{oct} = f_1(\sigma_m) \quad (12)$$

where $\sigma_m=(\sigma_1+ \sigma_2+\sigma_3)/3$. The mentioned function f is a monotonically increasing function (Linear (ML), Exponential (ME) and Second order (MS)).

Hoek and Brown Criterion (1980): This empirical criterion uses the uniaxial compressive strength of the intact rock material as a scaling parameter, and introduces two dimensionless strength parameters, m and s. After studying a wide range of experimental data, Hoek and Brown (1980) stated that the relationship between the maximum and minimum stress is given by

$$\sigma_1 = \sigma_3 + C_0\sqrt{m\frac{\sigma_3}{C_0} + s} \quad (13)$$

m and s are constants that depend on the properties of the rock and on the extent to which it had been broken before being subjected to the failure stresses σ_1 and σ_3.

Applied Data

The two sets of triaxial tests data belong to well 7125/1-1 (depth ranges from 1363 to 1369 m) and 7228/9-1 (depth ranges from 1042 to 1044 m) respectively from the Barents Sea. The applied data that are presented in Table 1, are obtained by the Norwegian Geotechnical Institute (NGI) by performing triaxial tests on the available Hekkingen shale cores that acts as a seal for the lower reservoir layers of Stø formation. The performed tests are consolidated undrained (CU) shear tests. The four most common failure criteria have been applied to calculate the maximum effective principal stress (σ_1) that causes the shaly rocks to illustrate shear failure along a failure plane.

Table 1 *Applied data in the study from Hekkingen shales*

Test No.	Depth (m)	τ_{max} (MPa)	σ_{1max} (MPa)	σ_{3max} (MPa)	ε_{af} (%)	Mean Angle Degree (β)	Core Drilling Direction
Core Samples Group 1 (G_1)							
7	1363.73	20.7	49.4	8.8	1.0	56	Vertical
6	1363.73	19.7	54.7	15.3	0.6	57	Vertical
3	1363.00	24.7	80.7	31.3	1.1	52	Vertical
10	1360.80-1361	28.9	102.8	45.0	1.7	53	Vertical
4	1361.00-0.45	27.7	115.4	60.0	0.9	51	Vertical
9	1360.80-1361	29.0	128	70.0	0.8	50	Vertical
11	1369.00-0.27	30.2	77,1	16.7	0.9	74	Horizontal
12	1362.00-0.27	39.0	112,3	34.3	1.4	69	Horizontal
Core Samples Group 2 (G_2)							
2	1043.57-0.68	7,5	21,3	6,3	0.5	53	Vertical
1	1043.57-0.68	10,4	32,3	11,5	0.5	62	Vertical
6	1042.50-0.60	16	68,4	36,4	1.3	62	Vertical
4	1043.78-0.88	22,7	105,8	60,4	2.7	49	Vertical
5	1042.50-0.60	21,8	109	65,4	2.4	55	Vertical

The parameters S_0 and φ are obtained as 16 MPa and, 9 degrees and 7 MPa and, 8 degrees for horizontal samples of groups G_1 and G_2 respectively. For vertical samples belonging to G_1, parameters S_0 and φ are obtained as 8 MPa and, 23 degrees. The schematic representations of the Mohr-Coulomb Circles for these 2 groups are illustrated in figures 1a and 1b respectively.

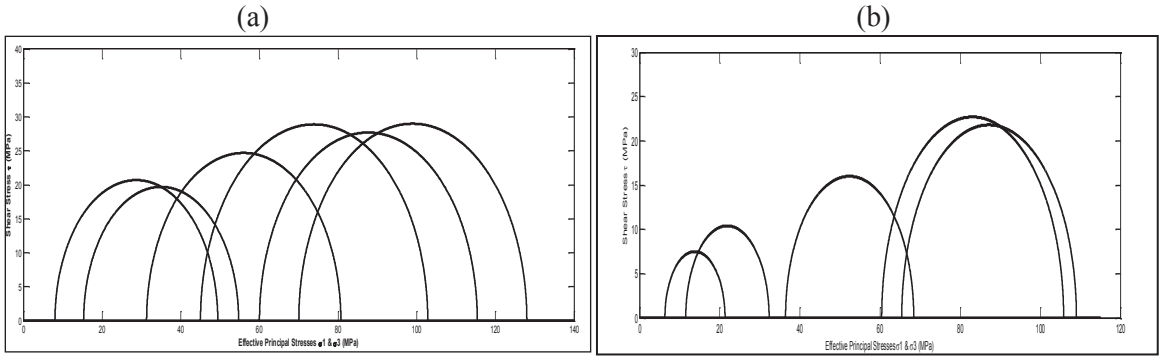

Figure 1 *Mohr Circles obtained from triaxial tests performed on shale samples belonging to a) G_1 and b) G_2*

Results and discussion

The predicted effective maximum principal stresses (σ_1) with different failure criteria versus observed maximum effective principal stresses have been shown in figures 2a and 2b for G_1 and G_2 respectively. Also, the observed amounts of average absolute error (AAE) for the prediction of σ_1 of two sets of shale samples have been demonstrated in figures 3a and 3b respectively. The applied formula for the calculation of AAE is as follows:

$$AAE = \frac{\left|\sigma_1^{calculated} - \sigma_1^{observed}\right|}{\sigma_1^{observed}} \qquad (14)$$

Based on Figures 2a and 3a, all the applied failure criteria except IDP have very good performance in predicting σ_1 of the shale samples of group G_1. The same statement can be applied for group G_2

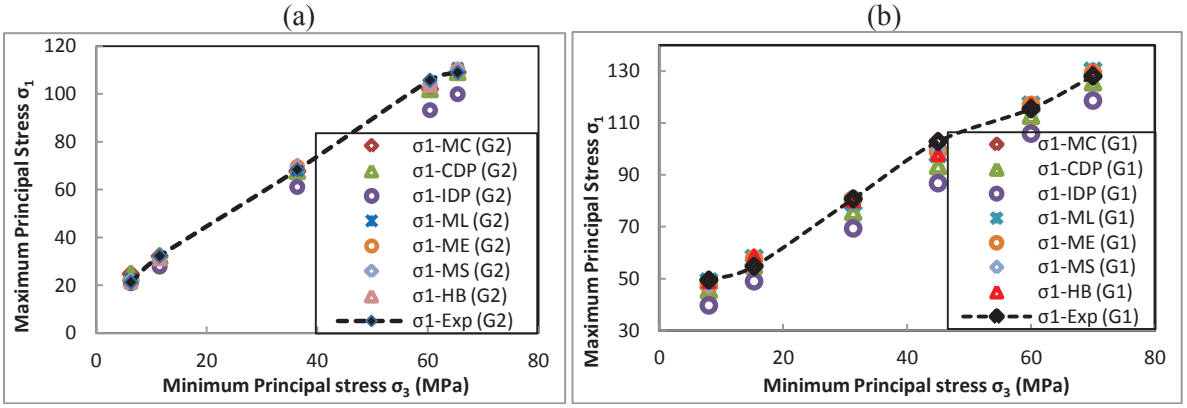

Figure 2 *Predicted maximum principal stresses versus minimum principal stresses for shales of a) group G_1 and b) group G_2 by different failure criteria.*

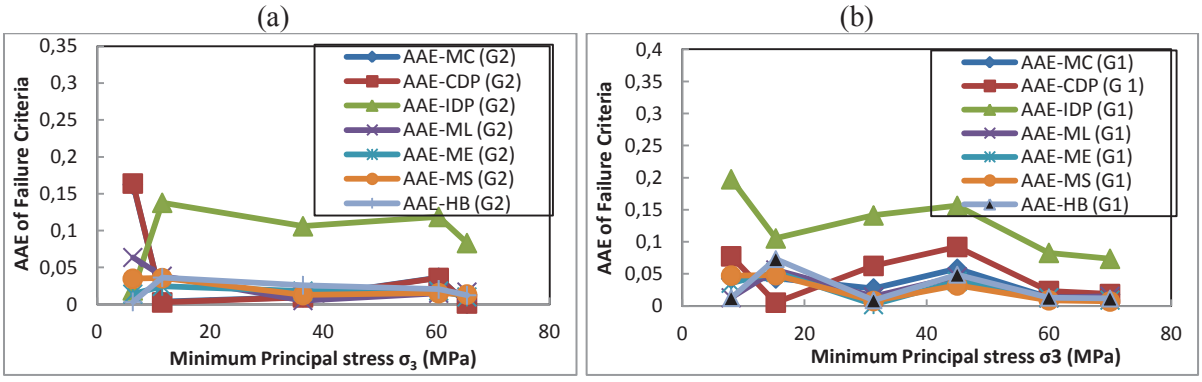

Figure 3 *Obtained AAE from different failure criteria for prediction of maximum principal stresses for Hekkingen shales of a) group G_1 and b) group G_2*

(Figures 2b and 3b). The maximum prediction error (AAE) for both cases has been occurred in case of applying IDP failure criterion while traditional Mohr-Coulomb criterion as the simplest failure

criterion has successfully predicted the σ_1 for both shale sample of groups G_1 and G_2 illustrated in Figures 3a and 3b respectively. The lower precision of the IDP and CDP criteria can be justified regarding that these criteria had been originally introduced for polyaxial shear tests in which two horizontal stresses are not equal. As in table 2 has been illustrated, the values of the correlation coefficients R^2 obtained from applying different failure criteria for the prediction of σ_1 are more than 98% that is acceptable. Also regarding Figures 2, 3 and table 2, applying second order and exponential terms in Mogi failure criterion, have improved the prediction performance of Mogi linear failure criterion for both sets of shale core samples. The obtained parameters S_0 and φ are different for horizontal and vertical shale samples of group G_1.

Table 2 *Obtained correlation coefficients (R^2) from applying different failure criteria for predicting σ_1 of the Hekkingen shales*

	MC	CDP	IDP	ML	ME	MS	HB
Group 1 (G_1)	0.989	0.989	0.989	0.993	0.994	0.995	0.991
Group 2 (G_2)	0.998	0.997	0.997	0.998	0.999	0.999	0.998

Conclusions

In this study four most common failure criteria have been utilized to predict the maximum effective principal stress (σ_1) of Hekkingen shale cores from two wells from the Barents Sea tested under triaxial consolidated undrained shearing conditions. A comparison of the obtained results reveals that popular Mohr-Coulomb (MC) has successfully predicted the σ_1 with high correlation coefficient of R^2=0.99. This means that MC criterion can surely be applied for uniaxial and triaxial test calculations. Also the best prediction results with lowest AAE and highest correlation coefficients are obtained by applying Mogi failure criterion. By applying exponential and second order functions the Mogi prediction has improved the precision. The lowest degrees of precision are due to applying Drucker-Prager failure criterion and this problem can be justified regarding that the IDP and CDP are presented specifically for poly axial shear testing. The observed discrepancies between the obtained parameters S_0 and φ for horizontal and vertical shale core samples of group G_1 reveals an anisotropy in the mechanical properties of the Hekkingen shales.

Acknowledgements

This work is a part of the SUCCESS (Subsurface CO_2 Storage, Critical Elements and Superior Strategy) and BarRock projects funded by Research Council of Norway and has been performed at the University of Oslo and the Norwegian Geotechnical Institute. We thank statoil for permission to publish the data. I thank my supervisors; Per Aagaard, Nazmul H. Mondol and Fabrice Cuisiat for the profound assistance and maturation of this research.

References

Fjær, E., Holt, R.M., Horsrud, P., Raaen, A.M., Risnes, R. [1992] Petroleum related rock mechanics. *Elsevier Science Publishers, Amsterdam, Netherlands.*

Hoek, E. and Brown, E.T. [1980] Empirical strength criterion for rock masses. *Journal of the Geotechnical Engineering Division,* **106**, 1013-1035.

McLean, M.R. and Addis, M.A. [1990] Wellbore Stability: The Effect of Strength Criteria on Mud

Mogi, K. [1971] Effect of the triaxial stress system on the failure of dolomite and limestone, *Tectonophysics*, **11 (2)**, 111-127

Rawlings, C.G. and Chryssanthakis, P. [1990a] Rock strength and zero lateral strain triaxial tests on cap rock, Well 7125/1-1, Barents Sea. *NGI Report no. 896506-1*, 1-30.

Rawlings, C.G., Chryssanthakis, P., 1990b. Rock strength and zero lateral strain triaxial tests on cap rock, Well 7228/9-1, Barents Sea. *NGI Report no. 901026-1*, 1-30.

Extended Abstract II

Seismic response of CO_2 saturated Red Wildmoor Sandstone under varying temperatures and pressures

By:

Javad Naseryan Moghadam, Nazmul Haque Mondol, Øistein Johnsen, Helge Hellevang and Per Aagaard

76th EAGE Conference & Exhibition 2014, 16-19 June 2014, Amsterdam, Netherlands

(DOI: 10.3997/2214-4609.20140849)

Amsterdam '14

Tu G107 15

Seismic Response of CO2 Saturated Red Wildmoor Sandstone under Varying Temperatures and Pressures

J. Naseryan Moghadam* (University of Oslo), N. Haque Mondol (University of Oslo), H. Hellevang (University of Oslo), Ø. Johnsen (Norwegian Geotechnical Institute) & P. Aagaard (University of Oslo)

SUMMARY

Underground geological sequestration of CO2 is considered as one of the most promising solutions for overcoming the global warming problem. Time lapse seismic monitoring enables us to monitor the CO2 plume migration and is considered as an integral component of a geological CO2 sequestration project because the seismic behavior of the rock is a function of both mineralogical composition and also the physical properties of the pore fluids. CO2 can be presented as gaseous, liquid and supercritical states at the uppermost kilometer of the sedimentary basin while in CO2 sequestration operation the supercritical and liquid states of CO2 are preferred due to the higher sweep efficiency. In this study, both compressional (Vp) and shear (Vs) wave velocities of a CO2 saturated Red Wildmoor sandstone sample under different temperature and pressure conditions are measured in a uniaxial hydrostatic cell equipped with acoustic transmitting and receiving transducers. The observed velocities illustrate that by introducing CO2 into the dry core, the resultant wave velocities decrease up until the critical condition in which by further increasing the CO2 pressure the Vs remains unchanged while the Vp gradually increases up to the maximum pressured applied in this study. Also it was observed that at lower temperature, the gas to liquid CO2 phase transition occurs with a sudden decrease in the amounts of the observed velocities while at higher temperature the velocity reduction is smoother possibly due to reaching the supercritical state. The observed velocities are in good agreement with Gassmann predicted velocities as well as literature data.

Introduction

Global warming due to anthropogenic release of CO_2 into the atmosphere is one of the most challenging environmental issues during recent years. One of the proposed solutions for resolving this problem is subsurface sequestration of anthropogenic CO_2 emissions. The subsurface injected CO_2 should be trapped inside the target reservoir formation for a considerable long period of time, otherwise the buoyant CO_2 returns to the atmosphere and surrounding formations and the success of CO_2 sequestration operation will be under question. Monitoring is one of the most important parts during CO_2 sequestration projects and is crucial in order to make sure about the containment of the stored CO_2 inside the target reservoir. Seismic monitoring is considered as an integral component of a controlling program at any geological exploration and sequestration project because the seismic behaviour of the geological formation can be affected by mineralogical composition and petrophysical properties of the target formation, and also the pore fluid properties. Applying seismic survey can be utilized for tracking the sequestrated CO_2 plume movement. Rock physical properties of CO_2 like bulk modulus and fluid density are noticeably different from the physical properties of formation brine and oil and therefore injecting CO_2 into the target reservoir formation regardless of its present thermodynamic phase will result in considerable alteration of seismic signature of the storage formation that makes the qualitative monitoring of the sequestrated CO_2 possible. The acoustic velocity response of a porous medium saturated with pore fluid, is a function of rock elasticity, porosity, pore fluid density and fluid bulk modulus. The mentioned acoustic velocity components can be affected by the temperature, rock mass stresses, pore fluid pressure and composition. In case of CO_2 sequestration, the injected CO_2 will displace the brine or oil and the resultant pore medium seismic behaviour has been studied at several publications (Gutierrez et al., 2012, Shi et al., 2007). CO_2 can be present in reservoir conditions in 3 phases as gaseous, liquid and supercritical states in contrast with typical reservoir pore fluids. The mentioned CO_2 phase transition phenomenon can make the study and interpretation of the acquired seismic signals challenging. CO_2 is preferred to be handled in liquid and supercritical phases due to easier handling and more economic transportation and also more efficient storage of CO_2 into subsurface formation due to the higher viscosity and sweep efficiency. In this study, the effect of CO_2 phase transition on acoustic signature of a well known sandstone core has been investigated at different temperature and pressure conditions.

Properties of CO_2 thermodynamic phases

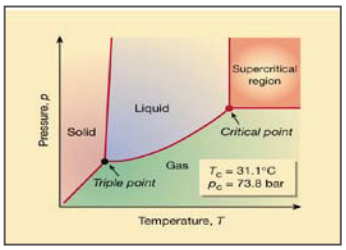

Figure 1: CO_2 Thermodynamic phases (Leitner., 2000)

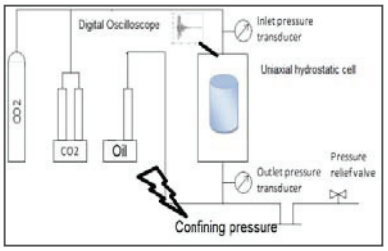

Figure 2: Experimental uniaxial hydrostatic setup utilized in this experiment

In figure 1, the phase diagram of pure CO_2 is illustrated (Leitner, 2000). The accepted critical temperature and pressure for CO_2 are 31.1 °C and 7.3 MPa respectively (Leitner, 2000). Supercritical CO_2 has physical properties of both liquid and gaseous CO_2 and is normally preferred for the sequestration purposes for ease o f handling and higher sweep efficiency. The CO_2 liquid-gas transition can occur at temperatures and pressures that are accessible within the first kilometre of sedimentary basin. Within the supercritical region however, the change in physical properties of CO2 are gradual and continuous, in contrast to the abrupt changes when crossing the gas-liquid boundary.
The Gassmann's fluid substitution is one of the most widely used fluid substitution equations in rock physics. It states that the bulk modulus of a saturated rock (K_{sat}) is related to the bulk modulus of rock frame (K_{dry}), the mineral grain bulk modulus (K_s), the bulk modulus of the pore fluid (K_f) and the rock porosity (Gassmann, 1951).

$$\frac{K_{sat}}{K_s - K_{sat}} = \frac{K_{dry}}{K_s - K_{dry}} + \frac{K_f}{\varphi(K_s - K_f)} \qquad \text{(eq 1)}$$

The bulk modulus of a rock that is saturated by fluid 1 can be calculated when we know the elastic properties of the same rock that is saturated with the fluid number 2 (Mavko et al., 2009):

$$\frac{K_{sat1}}{K_s - K_{sat1}} - \frac{K_{f1}}{\varphi(K_s - K_{f1})} = \frac{K_{sat2}}{K_s - K_{sat2}} - \frac{K_{f2}}{\varphi(K_s - K_{f2})} \qquad (eq\ 2)$$

Fluids cannot sustain shear forces, so the shear modulus of a saturated rock is the same as the dry rock:

$$\mu_{sat} = \mu_{dry} \qquad (eq\ 3)$$

and for determining the seismic velocities of a saturated rock we use following relations:

$$V_p = \sqrt{\frac{K_{sat}+4/3\mu}{\rho_{sat}}} \qquad (eq\ 4) \qquad\qquad V_s = \sqrt{\frac{\mu}{\rho_{sat}}} \qquad (eq\ 5)$$

In which the saturated density of the rock is defined as:

$$\rho_{sat} = (1-\varphi)\rho_s + \varphi\rho_f \qquad (eq\ 6)$$

In this relation, ρ_s and ρ_f are solid grain and pore fluid densities respectively. For calculating the mineral grain bulk modulus, the quantitative mineralogy of the core sample must be identified. In this study the available data from Spears (1983) for mineralogy and Bass (1995) for determining grain bulk modulus of Red Wildmoor sandstone have been utilized (table 1).

Minerals	Percentage	Ks (GPa)
Quartz	79%	37.8
K-Feldspar	19%	55.4
Albite	2%	56.9

Table 1: The mineralogical composition and solid grain bulk modulus of Red Wildmoor sandstone

For determining the representative value for solid grain bulk modulus, the Hill's average (1952) is applied:

$$K_s = 1/2(K_v + K_r) \quad (eq\ 7)$$

$$Kv = \sum_{i=1}^{N} f_i K_i \ \ (Voigt's\ average) \ (eq\ 8) \qquad\qquad \frac{1}{Kr} = \sum_{i=1}^{N} \frac{f_i}{K_i} \ (Reuss's\ average) \ (eq\ 9)$$

The CO_2 physical properties like sound velocity (V_f) and density (ρ_f) at different thermodynamic conditions are extracted from the online National Institute of Standards and Technology (NIST) chemical web-book and the CO_2 bulk modulus K_f is calculated by utilizing the following equation:

$$K_f = \rho_f V_f^2 \quad (eq\ 10)$$

After calculating the core saturated bulk modulus at different temperature and pressure conditions, the expected seismic velocities are calculated and are compared with the observed seismic velocities.

Experimental procedure

In this study the ultrasonic pulse transmission technique wes used to acquire acoustic velocity of a Red Wildmoor Sandstone core with the length of 6.9 cm, diameter of 2.5 cm and average porosity of 27% that was fully saturated with CO_2 and. Both V_p and V_s were measured under different temperature and pressure conditions. The selected temperature and pressure range are representative of the in situ conditions of reservoir formation at which CO_2 can be both gas, liquid and supercritical states. The applied temperatures were 22, 30 and 40ºC and at each constant temperature, a series of velocity measurement from 1 to 17 MPa with 1 MPa pressure increment per step were performed. The CO_2 experiments were performed at Norwegian Geotechnical institute (NGI) by utilizing a uniaxial hydrostatic cell that is capable of providing confining-pore pressure and temperature up to 30 MPa and 80ºC respectively. The hydrostatic uniaxial cell is equipped with radial and axial mechanical deformation sensors that enable us to calculate the length and porosity of the core sample under different stress conditions. The schematic representation of the uniaxial hydrostatic setup is illustrated in figure 2. The hydrostatic confining pressure was provided by a GDS pump. The pore pressure was provided by 2 ISCO pumps that were able to function in both constant pressure and constant rate modes. The uniaxial cell was placed inside an isothermal cabin and before running high temperature runs, the whole system was heated and left over two full days to ensure a uniform temperature distribution all around the system. In order to make sure that the observed velocity alteration of the sample is only due to the CO_2 phase transition phenomenon and not the mechanical deformation of the sample, a constant effective stress of 4 MPa was applied to avoid the pore pressure build up effect. The core was placed inside a rubber sleeve equipped with transmitting and receiving transducers that are made of P- and S- piezoelectric ceramics. The transmitting transducer was excited by a 200 V fast rising square wave from a pulse generator and the induced signal was recorded by a digital

oscilloscope system. The final waveform was the stack of over 64 traces for minimizing the effect of random noises. In order perfectly seal the core, vacuum grease and a number of rubber seal AFLAS rings were applied on both ends of the sleeve. The whole assembly was placed inside a pressure cylinder that was filled with silicon oil (Polysiloxane) to provide a hydrostatic confining pressure all around the system.

Results

The obtained results illustrate that with increasing CO_2 pressure up until critical pressure and regardless of the applied temperature, a visible gradual reduction in the amounts of the observed V_p values can be detected. The observed reduction around the critical pressure is more catastrophic up to 150 m/s (6%) that can be interpreted as clear indication of CO_2 phase transition (Figure 3). After exceeding the critical pressure, the observed CO_2 V_p is first rather stable and then increases slightly. Shear wave velocity (V_s) shows the same decreasing trend up to the critical pressure. Increasing the CO_2 pressure past the critical point, does not affect the observed V_s values (Figure 4). It can be justified by regarding the fact that by introducing CO_2 into the sample, firstly a sudden decrease in the amount of the rock bulk modulus occurs that causes the compressional waves to move slower inside the rock. With increasing the CO_2 pressure, both rock bulk modulus and bulk density increase till critical pressure condition, but the effect of density dominates the effect of rock bulk modulus and based on equation (4) the overall velocity decreases. Past critical pressure, the effect of rock bulk modulus increment is larger than the effect of rock bulk density increment. The observed V_p values exhibit a gradual increase, being in agreement with the predicted velocity values by Gassmann's equation and general behavior of CO_2 obtained from thermodynamic recourses (NIST). Based on equation 5, the shear wave velocity is just a function of rock shear modulus and because the shear modulus of the rock remains unchanged, increasing the rock bulk modulus will result in gradual reduction of the observed V_s values up to critical pressure and a constant behavior past critical condition.

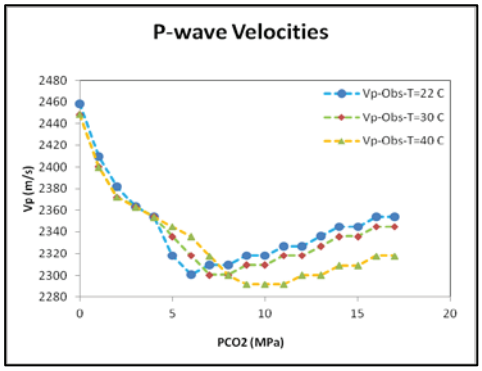

Figure 3: The observed V_p values at different T and P conditions

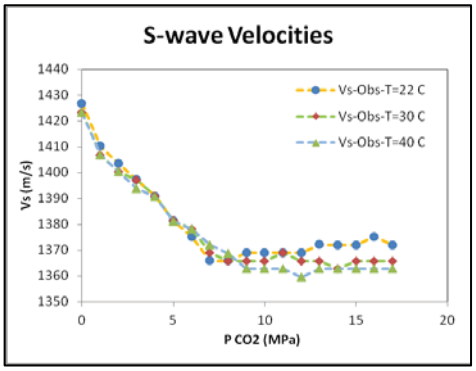

Figure 4: The observed V_s values at different T and P conditions

In the runs at higher temperature (T=40 ºC), the V_p and V_s measurements showed that the CO_2 phase transition occurs at higher pressures (between 7-9 MPa) compared to the low temperature runs (T=22 ºC) where it occurs between 4-6 MPa. The observed phenomenon is in total agreement with the thermodynamic behavior of CO_2 under different temperature and pressure conditions (Span et al., 1996). It was also observed that at higher temperatures, where CO_2 goes from gaseous to super critical conditions, the induced velocity reduction is smoother compared to the sharper velocity reduction trend at the lower temperature runs that passes liquid-gas phase boundary. It can be justified by regarding the fact that physical properties of CO_2, like bulk modulus and density, exhibit gradual changes going from gaseous to supercritical conditions. The same seismic behavior of the CO_2 saturated rock is reported by Yam (2011). The observed CO_2 seismic velocities are in good agreement with the obtained velocity values derived from Gassmann's fluid substitution equation that is utilized for calculation of core acoustic velocities under different CO_2 temperature and pressure conditions. The predicted V_p and V_s velocities by Gassmann equations for different temperatures are illustrated in figures 5 and 6 respectively.

5a 5b 5c

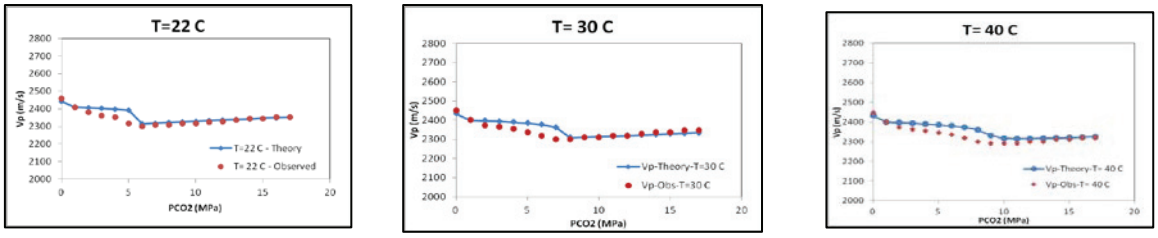

Figure 5: The observed and predicted V_p values for Red Wildmoor sandstone at temperatures a) 22°C, b) 30°C and c) 40°C

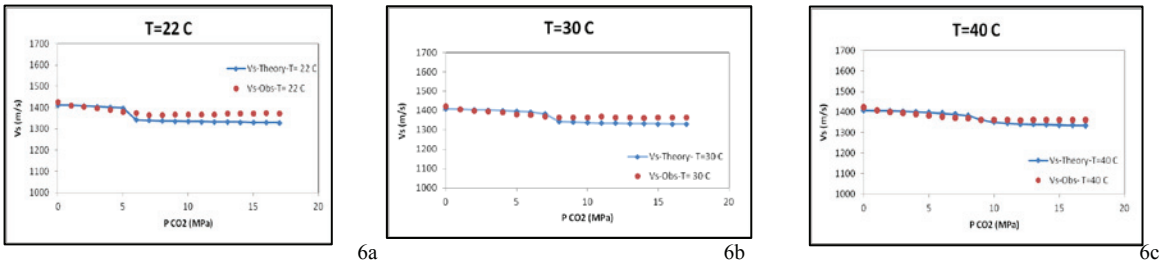

6a 6b 6c

Figure 6: The observed and predicted V_s values for Red Wildmoor sandstone at temperatures a) 22°C, b) 30°C and c) 40°C

Conclusions

It has been observed that introducing CO_2 regardless of its temperature, will reduce the wave velocity of the rock up t o the critical pressure. Past critical condition, the shear wave velocity remains unchanged due to its independency to rock bulk modulus, while the V_p gradually increases with increasing pressure. The velocity reduction around 5-6% observed during the CO_2 pressure increment at each selected temperature. This phenomena is observed almost at the same interval that was predicted to be the CO_2 phase transition and can be regarded as a clear indication of reaching phase boundary. The observed velocities are in good a greement with the calculated velocity using the Gassmann's equation. In the real reservoir formations, injected CO_2 will be stored together with initial pore fluids, and may not reach fully saturation. However, as it can be analyzed having an end member of fully CO_2 saturation (100%), assisting in a b etter interpretation of 4D seismic data to estimate saturation of injected CO_2.

Acknowledgements

This work is a part of the SUCCESS (Subsurface CO_2 Storage, Critical Elements and Superior Strategy) project funded by the Research Council of Norway and has been performed at the University of Oslo and the Norwegian Geotechnical Institute (NGI).

References

Bass, J. D., [1995], Elasticity of Minerals, Glasses, and Melts, *in* T. J. Ahrens, ed., Mineral physics and crystallography: A Handbook of Physical Constants. American Geophysical Union, Washington, USA., pp 45-63.

Gassmann, F., [1951], Elasticity of porous media: Uber die Elastizitat poroser Medien. Vierteljahrsschrift der Naturforschenden Gesselschaft in Zurich, **96**, pp 1-23.

Leitner, W., [2000], Green chemistry: Designed to dissolve. Nature, 405, pp 129-130

Online National Institute of Standards and Technology (NIST) chemical web-book, http://webbook.nist.gov

Mavko, G., Mukerji, T., Dvorkin, J., [2009], The Rock Physics handbook, tools for seismic analysis of porous media. Cambridge University Press, pp 266-295

Shi, J., Xue, Z., Durucan, S., [2007], Seismic monitoring and modeling of supercritical CO_2 injection into a water-saturated sandstone: Interpretation of P-wave velocity data. International Journal of Greenhouse Gas Control, 1, 1750-5836, pp 473-480

Span, R., and Wagner, W., [1996] A new equation of state for carbon dioxide covering the fluid region from the triple-point temperature to 1100 K at pressures up to 800 MPa,"J. Phys. Chem. Ref. Data, Vol. 25, No. 6, pp. 1509–1596.

Spears, D. A. (n.d.). [1983], Geochemistry and mineralogy of Triassic sandstones and implications for groundw ater composition: Mineralogical Magazine 47, (2), 183-190

Reuss, A., [1929], Berechnung der fliessgrense von m ischkristallen auf grund der plastizitatbedingung fur e inkristalle: Zeitschrift fur Angewandte Mathematik aus Mechnik, **9**, 49-58.

Voigt, W., 1928, Lehrbuch der Kristallphysik: Teubner.

Yam, H., [2011], CO2 Rock Physics: A laboratory study. Recovery, CSPG CSEG CWLS Convention

Extended Abstract III

Determination of the effective stress coefficient for the permeability of two low permeable sandstones in the Svalbard area

By:

Javad Naseryan Moghadam, Nazmul Haque Mondol, Helge Hellevang and Per Aagaard

4th Low Permeability Workshop, 29-30 September 2014, Ecole Centrale de Lille, France

Determination of the effective stress coefficient for the permeability of two low permeable sandstones in the Svalbard area

J. Naseryan Moghadam [1], N.H. Mondol [1,2], H. Hellevang [1], P. Aagaard [1]

Address: [1] *Department of Geosciences, University of Oslo, Norway*
Address: [2] *Norwegian Geotechnical Institutte (NGI), Oslo, Norway*

Email: j.n.moghadam@geo.uio.no

TOPIC:
1) Technical aspects of testing;
2) Procedures utilized;
3) Evaluation/interpretation of observations;
4) Standardization of parameters;

ABSTRACT:

Permeability is one of the most important petrophysical properties of rock that plays an important role in petroleum exploitation and CO_2 sequestration. Increasing the CO_2 injection pressure will influence the rock permeability. In order to analyze the effect of increasing pore pressure besides confining pressure, the parameter of the effective-stress coefficient for the permeability of the rock has been considered. The main objective of the study is applying the AFS-200 HP-HT flow system to determine the effective-stress coefficient for the permeability of two sandstones (Knorringfjellet (KN) and DeGeerdalen (DG) formations) from the Svalbard. The mentioned formations are considered as potential reservoirs for CO_2 sequestration in the Svalbard Island. The effective stress is defined as $\sigma_{eff} = \sigma_c - \alpha_k P_p$ in which σ_c is the confining stress around the rock and P_p is the pore fluid pressure. The α_k is the effective-stress coefficient for the permeability that states the contribution of pore pressure in permeability change of the rock compared to the effect of confining pressure around the core. Each physical quantity of rock has unique effective stress coefficient, and so by assuming the same for the permeability of rock (K) we will have:

$$K = K(\sigma_{eff}) = K(\sigma_c - \alpha_k P_p) \quad (1)$$

and

$$\alpha_k = -\frac{\left(\frac{\partial K}{\partial P_p}\right)_{\sigma_c}}{\left(\frac{\partial K}{\partial \sigma_c}\right)_{P_p}} \quad (2)$$

In this study, the cross-plot method (Walsh 1981) for determination of the α_k coefficient has been applied. First the core permeability at different applied pore pressures and constant confining pressures were plotted. Then, the pore pressure data was cross-plotted as a function of applied confining pressures for constant permeability values. The α_k coefficient then was calculated from the slop of the curve. The obtained results for the DeGeerdalen and Knorringfjellet core plugs are presented in figures 1 (a-b) and 1 (c-d) respectively.

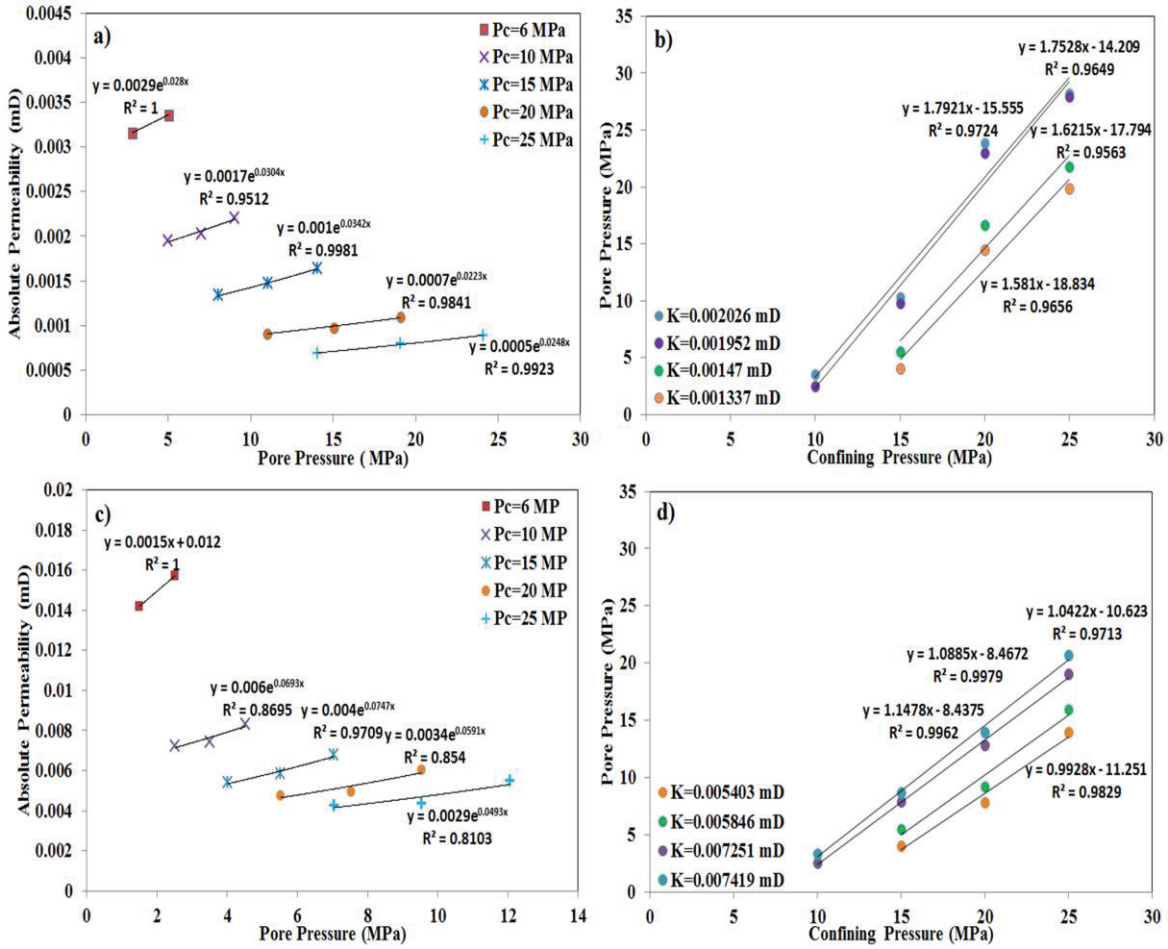

Figure 1: a) The obtained vertical permeability values at different P_p for constant σ_c (DG). b) σ_c - P_p cross-plot for DG core plug's iso-perm lines. c) The obtained vertical permeability values at different P_p for constant σ_c (KN). d) σ_c - P_p cross-plot for KN core plug's iso-perm lines.

The mentioned flooding system (AFS-200) is capable of providing reservoir in-situ conditions as high as temperature150^{0}C and pressure 70 MPa and also capable of running single phase and two phase relative permeability measurements (Figure 2).

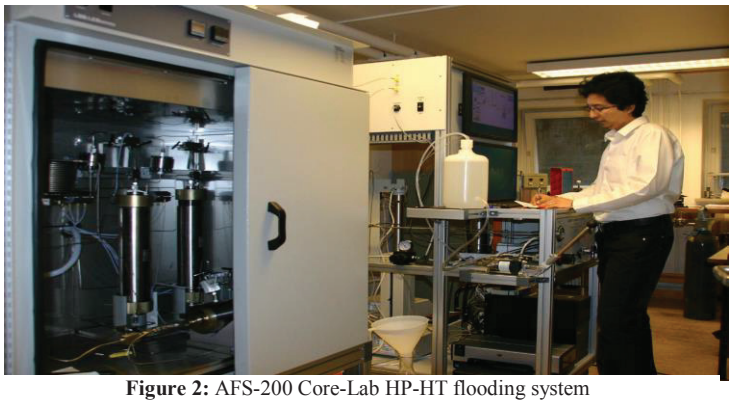

Figure 2: AFS-200 Core-Lab HP-HT flooding system

KEYWORDS:

Permeability, Effective stress, α_k coefficient, Confining stress, Pore pressure

DISCUSSION/MAIN CONTRIBUTIONS:

The obtained petrophysical properties from this study are in total agreement with the previous study (Farokhpour et al. 2010). The obtained porosity values for DG and KN sandstones are 0.08 and 0.14 respectively. The average calculated K_v for DG and KN at P_c=6 MP are 0.0035 and 0.015 mD respectively. The previously calculated permeabilities for these formations are 0.03 and 0.5 mD respectively ($K_v/K_h \approx 0.1$). The obtained α_k coefficients for the vertical permeability of these 2 sandstones are more than 1 (Table 1).

Core Sample	Medium P_c (10-20 MPa)	High P_c (15-25 MPa)
DeGeerdalen Sandstone	1.60	1.77
Knorringfjellet Sandstone	1.12	1.02

Table 1: The obtained effective stress coefficients for the permeability of DG and KN sandstones

Based on Berryman (1992), the α_k coefficient more than 1 reveals that the rock is not monomineralic. This is in total agreement with Mørk et al. (2011) that showed that these sandstones are composed of immature arkosic and lithic arenite dominated by plagioclase and quartz and detrital clay minerals like mica and chlorite. High values of the obtained α_k coefficients illustrate the important effect of pore pressure compared to confining pressure in rock permeability. Based on Walls (1982), the higher values of α_k coefficient can be attributed to the higher percentage of clays (Mørk et al. 2011) in the DG and KN sandstones. Clay minerals have higher compressibility compared to quartz and therefore are more sensitive to pore pressure compared to confining pressure. By increasing confining pressure, for both sandstone cores, the values of the obtained α_k's are decreased. It can be attributed to the fact that at high confining pressures, due to blockage of pore throat, the effect of pore pressure decreases and consequent α_k coefficient decreases.

References:

Berryman, J. G, (1992): Effective stress for transport properties of inhomogeneous porous rock, Journal of Geophysical Research. 97, 17409-17424.

Farokhpoor,R. Torsæter, O. Baghbanbashi, T. Mørk, A. and Lindeberg, E., (2010): Experimental and Numerical Simulation of CO_2 Injection Into Upper-Triassic Sandstones in Svalbard, Norway - SPE 139524, p.11

Mørk, M.B.E., (2011). Department of Geology and Mineral Resources Engineering, NTNU, Diagenesis and quartz cement distribution of low permeability Upper Triassic –Middle Jurassic reservoir sandstones, Longyearbyen CO2 Laboratory well site in Svalbard, Norway

Walls, J., and Nur, A., (1982). Pore pressure and confining pressure dependence of permeability in sandstone, Proceedings of the 7th Formation Evaluation Symposium of the CWLS, paper O, Canadian Well Logging Society, Alberta, Calgary.

Walsh, J., (1981). Effect of pore pressure and confining pressure on fracture permeability, International Journal of Rock Mechanics and Mining Sciences & Geomechanics Abstracts. 18(5), p. 429-435